

Faster Quantum Algorithms with “Fractional”-Truncated Series

Yue Wang¹ and Qi Zhao¹

¹*Department of Computer Science, University of Hong Kong, Pokfulam Road, Hong Kong*

(Dated: February 8, 2024)

Quantum algorithms frequently rely on truncated series approximations, necessitating a high truncation order to achieve even moderate accuracy and consequently resulting in intensive circuit complexity. In response, we propose a general framework, the Randomized Truncated Series (RTS), which offers two avenues for simplifying circuits: a quadratic improvement on the truncation error and enabling a continuously adjustable effective truncation order. The core idea is that the random mixing of two series of specific forms generates a substantial reduction in the truncation error. We present an error analysis for RTS with a new mixing lemma accounting for near-unitary operators. To demonstrate the effectiveness and versatility of RTS, we provide four illustrative examples within the context of Linear Combination of Unitary, Quantum Signal Processing, and solving Quantum Differential Equations. RTS shed light on the path towards practical quantum advantage.

Introduction.—Quantum computing holds the promise to redefine the limits of information processing. Quantum algorithms, such as those for Hamiltonian simulation (HS) [1–7], differential equation solving [8, 9], and singular value transformation [10, 11], achieve at most exponential asymptotic speedup compared to their classical counterparts [12]. These algorithms provide the computational power necessary for exploring complex systems, holding the potential to empower researches like quantum chemistry [13–18], condensed matter physics [19–21], cryptography [22], solving engineering problems [23–25] and finance [26].

One of the key components in quantum algorithms is implementing a polynomial transformation on an operator H . For instance, a Hamiltonian dynamics, e^{-iHt} can be approximated by either Taylor or Jacobi-Anger expansion [2–4]. Polynomials for other algorithms performing generalized amplitude amplification, matrix inversion, and factoring are illustrated in Ref. [3, 12]. In many of such algorithms, we truncate the polynomial at an integer order K with a truncation error δ . An increased K indicates higher precision but requires more qubits and gates, and a complicated circuit leads to vanishing quantum advantage [27, 28]. This challenge arises due to both the accumulation of physical errors over the long sequence of quantum gates and the lack of reliable error correction schemes. To implement an algorithm, K is derived according to the existing error analysis. Yet, the corresponding circuit is so complicated that harnessing from any quantum algorithm remains challenging. On top of that, data readout poses another obstacle. It was found that the number of samples required in HS scales exponentially with two-qubit gates presented in noisy circuits [29]. Therefore, even a constant reduction in circuit cost paves the way for practical quantum applications.

Cutting down circuit costs can be achieved if a simpler circuit does not compromise precision. A reduction on K can be achieved by optimizing the original algorithm [30, 31]. We also observe the potential to implement an algorithm with a fractional K , releasing the integer constraint, which incurs inefficiency during ceiling rounding

for K . In Fig. 1, when aiming for an algorithmic error $\epsilon_{target} = 10^{-2}$ in HS, choosing $K = 8$ results in $\epsilon = 1.17 \times 10^{-2}$. $K = 9$ boosts it to $\epsilon = 8 \times 10^{-4}$, which is significantly lower than the desired ϵ_{target} . Note that an overly accurate ϵ contributes little to the final accuracy when it is significantly lower than other errors like sampling bias and two-qubit gate infidelity. The ceiling rounding, which greatly reduces ϵ leads to wasteful allocation of resources. Therefore, designing the algorithm with a fractional K fine tunes ϵ at a specific level enhances gate efficiency.

In this letter, we introduce Randomized Truncated Series (RTS), a simple and general framework featuring random mixing, applicable for algorithms that depend on truncated polynomial functions. RTS results in a quadratically improved and continuously adjustable truncation error. The intuition comes from error cancellation in mixing polynomials. Consider a truncated series expansion, f_1 , with truncation error δ_1 . We can construct a higher-order polynomial, denoted as f_2 , in a way that the probability mixture of f_1 and f_2 with a probability $p \in [0, 1]$, expressed as $f_{\text{mix}} = pf_1 + (1-p)f_2$, exhibits a significantly reduced truncated error. This thought directly extends to mixing operators in quantum algorithms. We can construct two types of operators, V_1 and V_2 , analogous to f_1 and f_2 , respectively. Lemma 1 states the probability mixture of operators gives rise to a quadratic improvement in truncation error. Furthermore, we can make fine adjustments to the circuit cost by tuning the continuous p , essentially creating a fractional effective truncated order. The combined effect of the two improvements is remarkable. With the same gate budget, RTS improved the algorithmic error from 8.142×10^{-4} , as achieved by the original BCCKS algorithm [8], to 10^{-8} using RTS. This represents a remarkable $81425\times$ enhancement in ϵ . Such ϵ meet the demand for high-accuracy HS [32], where practical quantum advantages start to emerge.

RTS offers a versatile application for optimizing a variety of algorithms. We demonstrate a few in this letter: (I) Both the linear combination of unitary (LCU) [4] and quantum signal processing (QSP) [2] implementation

of HS. (II) Within the QSP framework, we also extend to the composition of other polynomials by considering the uniform spectral amplification (USA) [3]. (III) Complicated algorithms like solving differential equations [8] involving truncated series as subroutines. We are anticipating further generalizations on utilizing RTS in analog quantum computing and time-dependent evolution.

Framework.—Let's consider a familiar case to capture the essence of RTS. The Taylor expansion of unitary evolution under the system Hamiltonian H for time t can be written as

$$U = e^{-iHt} = \sum_{k=0}^{\infty} \frac{(-iHt)^k}{k!}. \quad (1)$$

We truncate Eq. (1) at integer order K_1 and define

$$F_1 := \sum_{k=0}^{K_1} \frac{(-iHt)^k}{k!}. \quad (2)$$

For the other polynomial, we find another integer $K_2 > K_1$ and construct

$$F_2 := \sum_{k=0}^{K_1} \frac{(-iHt)^k}{k!} + \frac{1}{1-p} \sum_{k=K_1+1}^{K_2} \frac{(-iHt)^k}{k!}. \quad (3)$$

Thus, $F_m := pF_1 + (1-p)F_2 = \sum_{k=0}^{K_2} (-iHt)^k / k!$ is exactly the Taylor's series truncated at K_2 , resulting in a much lower truncation error compared to both F_1 and F_2 . As we need resources linear with $K_{1(2)}$ to implement $F_{1(2)}$ [4, 33], implementing F_m acquire resources linear with $K_m := pK_1 + (1-p)K_2$. $p \in [0, 1]$ continuous modify K_m . Thus, we effectively truncate the overall series at a “fractional” order K_m , enabling fine adjustable circuit cost.

Although the evolution we are approximating is unitary, i.e. U in Eq. (1), the corresponding F_1 is only near-unitary due to the truncation. As elaborate in Appendix B, by choosing $p < 1 - \mathcal{O}(\epsilon)$, F_2 can also be near-unitary. We can thus approximate them by quantum circuits, V_1 and V_2 , with high probability. The failure probability of RTS depends on the algorithm we are applying to. Let the failure probability of carrying out V_1 be denoted as ξ_1 , and similarly, denote the failure probability of carrying out V_2 as ξ_2 , the overall failure probability of RTS is $(p\xi_1 + (1-p)\xi_2)$.

For clarity, we categorize algorithms based on circuit structure and address them in slightly different ways. Type 1 algorithms construct the quantum circuit by concatenating multiple identical segments, while Type 2 algorithms achieve the desired polynomial transformation without segmentation. It's important to note that while we can obtain the full quantum state for Type 1 algorithms, applying RTS to Type 2 algorithms allows retrieval of only classical information. Additionally, all errors, costs, and failure probabilities discussed in the following examples pertain to a single segment in Type

1 algorithms or the average behavior of the entire circuit for Type 2 algorithms. Here is the protocol to implement RTS for both types of algorithms.

RTS Protocol

1. A random generator returns the values 1 and 2 with the probability p and $(1-p)$ respectively;
2. Construct a quantum circuit $V_{1(2)}$ when the outcome in Step 1 is 1(2);
3. Based on the type of algorithm, either measure the concatenation of all circuits (type 1) or measure each of the quantum circuits separately (type 2);
4. Post-process the measurement results for the pre-determined sampling variance.

Mixing channel.—We renew the mixing lemma proposed in ref. [5, 34, 35] to be applicable for near-unitary dynamics (Proof in Appendix A). We begin by constructing a mixing channel \mathcal{V}_{mix} such that $\mathcal{V}_{\text{mix}}(\rho) = p\mathcal{V}_1(\rho) + (1-p)\mathcal{V}_2(\rho)$ for a density matrix ρ , where \mathcal{V}_1 and \mathcal{V}_2 are quantum channels corresponds to V_1 and V_2 respectively, i.e. $\mathcal{V}_{1(2)}(\rho) = V_{1(2)}\rho V_{1(2)}^\dagger$. $\mathcal{V}_{\text{mix}}(\rho)$ gives the expected outcome for RTS.

Lemma 1 (Non-unitary mixing lemma). *Let V_1 and V_2 be operators approximating an ideal operator U , and let the corresponding quantum channel be \mathcal{V}_1 and \mathcal{V}_2 . Denote the operator $V_m := pV_1 + (1-p)V_2$. Assume the operator norm $\|V_1 - U\| \leq a_1$, $\|V_2 - U\| \leq a_2$, and $\|V_m - U\| \leq b$, then the density operator $\rho = |\psi\rangle\langle\psi|$ acted by the mixed channel \mathcal{V}_{mix} satisfies*

$$\|\mathcal{V}_{\text{mix}}(\rho) - U\rho U^\dagger\|_1 \leq 2\varepsilon, \quad (4)$$

where $\varepsilon = 2b + pa_1^2 + (1-p)a_2^2$ and $\|\cdot\|_1$ is the 1-norm.

We will then demonstrate how to utilize RTS and the performances with several examples. In each example, we redefine variables to avoid using lengthy subscripts.

BCCKS example.—Hamiltonian simulation (HS) is one of the fundamental quantum algorithms. Moreover, it acts as subroutines in algorithms like Quantum Phase Estimation, Quantum Linear System Solver, etc. Therefore, accurate and efficient HS is crucial in both near- and long-term perspectives.

The BCCKS algorithm proposed in 2015 aims to implement Eq. (2). H can be decomposed into sum of unitaries H_l with coefficients α_l , i.e. $H = \sum_{l=1}^L \alpha_l H_l$. Then, we can re-express Eq. (2) and (3) as $F_1 \sum_{j=0}^{\Gamma-1} \beta_j \tilde{V}_j$ and $F_2 = \sum_{j=0}^{\Gamma'-1} \beta'_j \tilde{V}'_j$, where $\Gamma = \sum_{k=0}^K L^k$, $\Gamma' = \sum_{k=0}^{K_2} L^k$, $\tilde{V}_j^{(\prime)}$ represents one of the unitaries $(-i)^k H_{l_1} \cdots H_{l_k}$, and $\beta_j^{(\prime)}$ is the corresponding positive coefficient.

The form of F_1 and F_2 is a standard LCU [36] which can be implemented by **SELECT** and **PREPARE**

oracles followed by Oblivious Amplitude Amplification (OAA) [37]. For implementation details, one can refer [4, 33] and Appendix B.

Parallel to amplifying success probability, OAA also introduces excess errors due to $F_{1(2)}F_{1(2)}^\dagger \neq 1$. To quantify these errors, we need to explore the exact operator performed by $V_{1(2)}$. Similar to the BCCKS algorithm, we set $s := \sum_{j=0}^{\infty} \beta_j = 2$ by splitting the whole evolution into $r = (\sum_{l=1}^L \alpha_l t) / \log 2$ segments. Then, the evolution time of each segment, whether it be V_1 or V_2 , is $\tau = t/r$. In the last segment, which has an evolution time less than τ , we can compensate for the error by introducing another ancillary qubit [37]. For V_1 with $s_1 := \sum_{j=0}^{\Gamma-1} \beta_j$, this treatment is appropriately valid since $s_1 \approx 2$. However, the coefficients of extra terms in V_2 depend on p . Hence $s_2 := \sum_{j=0}^{\Gamma'-1} \beta'_j$ will deviate from 2 when p approaches 1. Our solution is to insert the condition $p \leq 1 - \mathcal{O}(\epsilon)$ and amplify V_2 by \mathfrak{s}/s_2 , where $\mathfrak{s} = \sin(\pi/10)^{-1}$. Resulting in $s_2 \approx \mathfrak{s}$. As constant commutes with all operators, we can always recover the constant amplification at the end of the algorithm. Consequently, a modified OAA, differing from what was implemented in the BCCKS algorithm, boosts the success probability of V_2 to near unity.

After OAA, quantum circuits implementing $F_{1(2)}$ performing the transform

$$\begin{aligned} |0\rangle |\psi\rangle &\mapsto |0\rangle V_{1(2)} |\psi\rangle + |\perp_{1(2)}\rangle \\ V_1 &:= \frac{3}{s_1} F_1 - \frac{4}{s_1^3} F_1 F_1^\dagger F_1 \\ V_2 &:= \frac{5}{s_2} F_2 - \frac{20}{s_2^3} F_2 F_2^\dagger F_2 + \frac{16}{s_2^5} F_2 F_2^\dagger F_2 F_2^\dagger F_2, \end{aligned} \quad (5)$$

where $(\mathbb{1} \otimes \langle 0 |) |\perp_{1(2)}\rangle = 0$. Thus, projecting on $|0\rangle$ in the first register by post-selection essentially implement $V_{1(2)}$. We interchangeably infer $V_{1(2)}$ as the operator in Eq. (5) and the quantum circuit performing the transformation. As the quantum circuits implement $V_{1(2)}$ with high probability, this does not pose confusion. The error bound, cost [4], and failure probability for RTS implementing the BCCKS algorithm is given by the following theorem (Proof in Appendix B).

Theorem 1. For V_1 and V_2 defined in Eq. (5), a mixing probability $p \in [0, 1)$ and a density matrix $\rho = |\psi\rangle\langle\psi|$, the evolved state under the mixing channel $\mathcal{V}_{\text{mix}}(\rho) = pV_1\rho V_1^\dagger + (1-p)V_2\rho V_2^\dagger$ and an ideal evolution for a segment, $U = e^{-iH\tau}$, is bounded by

$$\|\mathcal{V}_{\text{mix}}(\rho) - U\rho U^\dagger\| \leq \max \left\{ \frac{40}{1-p} \delta_1^2, 8\delta_m \right\}, \quad (6)$$

where $\delta_1 = 2^{\frac{(\ln 2)^{K_1+1}}{(K_1+1)!}}$ and $\delta_m = 2^{\frac{(\ln 2)^{K_2+1}}{(K_2+1)!}}$. The overall cost of implementing this segment is

$$G = \tilde{\mathcal{O}}(nL(pK_1 + (1-p)K_2)), \quad (7)$$

where n is number of qubit, L is the number of terms in the unitary expansion of H , and K_1 and K_2 are truncation order in V_1 and V_2 respectively. The failure probability corresponds to one segment being upper bounded by $\xi \leq \frac{8}{1-p} \delta_1^2 + 4\delta_1$.

Quantum Signal Processing examples (QSP).—QSP is powerful in transforming the eigenvalue of a Hermitian matrix H . We will demonstrate the application of RTS in two algorithms, which perform exponential function and truncated linear function transformations. Other algorithms relying on QSP can be addressed similarly. QSP can either be a Type 1 or Type 2 algorithm. Type 1 QSP sacrifices some constant overhead for classical computation hardness as it solves a lower-degree system of equations.

Consider a single eigenstate $|\lambda\rangle$ of H . QSP perform a degree- d polynomial transformation $f(\lambda)$ by classically finding a vector of angles $\vec{\phi} \in \mathbb{R}^d$ and construct an iterator $W_{\vec{\phi}}$ such that

$$\begin{aligned} W_{\vec{\phi}} &= \prod_{k \geq 1} Z_{\phi_k} W_\lambda Z_{\phi_k}^* = \begin{pmatrix} f(\lambda) & \cdot \\ \cdot & \cdot \end{pmatrix} \\ Z_{\phi_k} &= \begin{pmatrix} -ie^{-i\phi} & 0 \\ 0 & -1 \end{pmatrix} \\ W_\lambda &= \begin{pmatrix} \lambda & -\sqrt{1-|\lambda|^2} \\ \sqrt{1-|\lambda|^2} & \lambda \end{pmatrix}, \end{aligned} \quad (8)$$

where $Z_{\phi_k}^*$ is the complex conjugate of Z_{ϕ_k} . The notation is consistent with Ref. [2], and a self-contained derivation can also be found in Appendix C.

Regarding HS, we use $f(\lambda)$ to approximate $U_\lambda := e^{-i\lambda t}$ by the truncated Jacobi-Anger expansion [38]. Specifically, there exist a $\vec{\phi}$ such that $f(\lambda)$ is the following function

$$\begin{aligned} U_{K_1}(\lambda) &= A_1(\lambda) + iC_1(\lambda) \\ A_1(\lambda) &:= J_0(t) + 2 \sum_{\text{even } k > 0}^{K_1} (-1)^{\frac{k}{2}} J_k(t) T_k(\lambda) \\ C_1(\lambda) &:= 2 \sum_{\text{odd } k > 0}^{K_1} (-1)^{\frac{k-1}{2}} J_k(t) T_k(\lambda), \end{aligned} \quad (9)$$

where $J_k(t)$ is the Bessel function of the first kind, $T_k(\lambda)$ is the Chebyshev polynomial. We then employ RTS to improve the algorithmic error. The following theorem gives new error bounds, costs, and failure probabilities (Proof in Appendix C follows from Ref. [2, 33] and lamma 1).

Theorem 2. (Informal) Regarding the quantum circuit implementing Eq. (9) as V_1 , there exist a V_2 with maximum degree $K_2 > K_1$ such that given a mixing probability $p \in [0, 1)$ and a density matrix $\rho = |\psi\rangle\langle\psi|$, distance between the evolved state under the mixing channel $\mathcal{V}_{\text{mix}}(\rho) = pV_1\rho V_1^\dagger + (1-p)V_2\rho V_2^\dagger$ and an evolution channel for U_λ is bounded by

$$\|\mathcal{V}_{\text{mix}}(\rho) - U_\lambda \rho U_\lambda^\dagger\| \leq \max \left\{ 28\delta_1, 8\sqrt{\delta_m} \right\}, \quad (10)$$

where $\delta_m = \frac{4t^{K_2}}{2^{K_2} K_2!}$ and $\delta_1 = \frac{4t^{K_1}}{2^{K_1} K_1!}$. The overall cost of implementing this segment is

$$G = \mathcal{O}(dt\|H\|_{max} + (pK_1 + (1-p)K_2)), \quad (11)$$

where d is the sparsity of H , and K_1 and K_2 are truncation order in V_1 and V_2 respectively. The failure probability is upper bounded by $\xi \leq 4p\sqrt{\delta_2}$.

The other algorithm we demonstrate under the context of QSP is the Uniform spectral amplification (USA) [3], which is a generalization of amplitude amplifications [37, 39] and spectral gap amplification [40]. This algorithm amplifies the eigenvalue by a factor of $1/2\Gamma$ if $|\lambda| \in [0, \Gamma]$ while maintaining H normalized. USA trying to implement the truncated linear function

$$f_{\Gamma, \delta}(\lambda) = \begin{cases} \frac{\lambda}{2\Gamma}, & |\lambda| \in [0, \Gamma] \\ \in [-1, 1], & |\lambda| \in (\Gamma, 1], \end{cases} \quad (12)$$

where $\delta = \max_{|x| \in [0, \Gamma]} \left| |x| \tilde{f}_{\Gamma}(\lambda) / (2\Gamma) - 1 \right|$ is the maximum error tolerance. Eq. (12) is approximated by $\tilde{f}_{\Gamma}(\lambda)$, formed by composing a truncated Jacobi-Anger expansion approximation of the error functions. Using RTS, error and circuit cost are given by the following theorems (Proof in Appendix C).

Theorem 3. (Informal) Regarding the quantum circuit implementing $\tilde{f}_{\Gamma}(\lambda)$ as V_1 , there exist a V_2 with maximum degree $K_2 > K_1$ such that given a mixing probability $p \in [0, 1)$ and a density matrix $\rho = |\psi\rangle\langle\psi|$, distance between the evolved state under the mixing channel $\mathcal{V}_{mix}(\rho) = pV_1\rho V_1^\dagger + (1-p)V_2\rho V_2^\dagger$ and an ideal transformation with Eq. (12) is bounded by

$$\|\mathcal{V}_{mix}(\rho) - f_{\Gamma, \delta}(\rho)\| \leq \max \left\{ 8b, \frac{4}{1-p}a_1^2 \right\}, \quad (13)$$

where $\hat{f}_{\Gamma, \delta}(\rho)$ is the ideal quantum channel, $a_1 = \frac{8\Gamma e^{-8\Gamma^2}}{\sqrt{\pi}} \frac{4(8\Gamma^2)^{K_1/2}}{2^{K_1/2}(K_1/2)!}$ and $b = \frac{8\Gamma e^{-8\Gamma^2}}{\sqrt{\pi}} \frac{4(8\Gamma^2)^{K_2/2}}{2^{K_2/2}(K_2/2)!}$. The overall cost of implementing this segment is

$$G = \mathcal{O}(dt\|H\|_{max} + (pK_1 + (1-p)K_2)), \quad (14)$$

where d is the sparsity of H , and K_1 and K_2 are truncation order in V_1 and V_2 respectively.

Ordinary Differential Equation example.—Solving differential equations [8, 9, 41, 42] is another promising application of quantum computing, empowering numerous applications.

Consider an anti-Hermitian operator A and the differential equation of the form $d\vec{x}/dt = A\vec{x} + \vec{b}$, where $A \in \mathbb{R}^{n \times n}$ and $\vec{b} \in \mathbb{R}^n$ are time-independent. The exact solution is given by

$$\vec{x}(t) = e^{At}\vec{x}(0) + (e^{At} - \mathbb{1})A^{-1}\vec{b}, \quad (15)$$

where $\mathbb{1}$ is the identity vector.

We can approximate e^z and $(e^z - \mathbb{1})z^{-1}$ by two K_1 -truncated Taylor expansions:

$$\begin{aligned} T_{K_1}(z) &:= \sum_{k=0}^{K_1} \frac{z^k}{k!} \approx e^z \\ S_{K_1}(z) &:= \sum_{k=1}^{K_1} \frac{z^{k-1}}{k!} \approx (e^z - 1)z^{-1}. \end{aligned} \quad (16)$$

Given non-negative integer j , denote x^j as the approximated solution at time jh for a short time step h with $x^0 = \vec{x}(0)$. We can calculate x^j by the recursive relation

$$x_1^j = T_{K_1}(Ah)x^{j-1} + S_{K_1}(Ah)\vec{b}. \quad (17)$$

Furthermore, we encode the series of recursive equations in a large linear system \mathcal{L}_1 as proposed in Ref. [8] and denote the quantum circuit solving the linear system as V_1 . Sampling results on V_1 give information of x^j for j . To employ RTS, we construct another circuit V_2 that encodes $x_2^j = T_{K_2}(Ah)x_2^{j-1} + S_{K_2}(Ah)\vec{b}$, where $T_{K_2}(z)$ and $S_{K_2}(z)$ are modified expansions with maximum order K_2 in another linear system \mathcal{L}_2 . RTS mixes the solution to \mathcal{L}_1 and \mathcal{L}_2 with probability p and $1-p$ respectively to give x_{mix}^j (Detailes in Appendix D).

Theorem 4. (Informal) Suppose x_{mix}^j are approximated solutions to Eq. (15) at time $t = jh$ using the random mixing framework. We can upper bound the estimation error by

$$\|\langle \bar{x}^j \rangle - |x(jh)\rangle\| \leq \max \left\{ 8b, \frac{4}{1-p}a_1^2 \right\}, \quad (18)$$

where $a_1 \leq \frac{C_j}{(K_1+1)!}$, and $b \leq \frac{C_j}{(K_2+1)!}$. C_j is a problem specific constant.

Numerical Results.—We analyze the error upper bounds and costs implement RTS on the BCCKS algorithm [4] simulating the Ising model for $t = 100$

$$H = \sum_{i=1}^n \sigma_i^x \sigma_{i+1}^x + \sum_{i=1}^n \sigma_i^z, \quad (19)$$

where σ_i are Pauli operators acting on the i^{th} qubit and $n = 100$. We separate the simulation into $r = \sum_i \alpha_{it}/\log(2) = 28854$ segments. To make a focused illustration of RTS, we make the following simplification: (I) We omit the time difference presented in the last segment as it makes a negligible difference; (II) Since the dominant gate cost is the **SELECT** oracle, we consider the **PREPARE** oracle as a free operation; (III) we assume the hermitian conjugate of **SELECT** can be implemented without extra cost.

Each segment performing $V_{1(2)}$ defined in Eq. (5) need 3(4) **SELECT**. Each of it can be implemented by $K(7.5 \times 2^w + 6w - 26)$ CNOT gates [33], where K is the

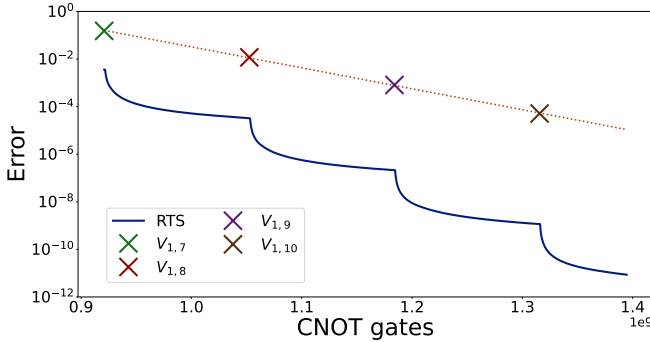


FIG. 1. Algorithmic error and corresponding CNOT gate cost. Cross markers with different colors correspond to the original BCCKS algorithm with discrete truncation, where we denote V_{1,K_1} for a K_1 -truncated V_1 quantum circuit. The solid blue line indicates the performance when employing RTS. Any point on the line corresponds to the error obtained by the optimal set of parameters $\{K_1, K_2, p\}$ using up all CNOT gates.

truncation order and $w = \log_2(L)$. For a fixed cost budget, we traverse all feasible sets $\{K_1, K_2, p\}$ that use up the budget and find the minimum $r\epsilon$, which is the final algorithmic error with RTS. The result is shown in Fig. 1, with crosses representing the performance under discrete truncation, and the blue line indicating the optimal error achieved at a specific cost using RTS. There are two features in Fig. 1 that manifest the advantages of RTS. Firstly, the blue line declines faster than the orange dotted line, which is the line fitting the 4 cross marks, meaning we greatly improved the accuracy. This in turn means we can use much less resources to achieve the target precision, which is crucial in implementing quantum algorithms on real devices. For example, targeting $\epsilon = 10^{-8}$, we save about 30% of CNOT gates. Secondly, the blue line is continuous opposite to 4 discrete points, suggesting we can always find a set $\{K_1, K_2, p\}$ that achieves a desired error without any waste.

Fig. 2 further explores the relationship between cost and error. The main figure shows the variation of cost for given V_{mix,K_1,K_2} with varying p . The sub-figure displays the error improvement for multiple V_{m,K_1,K_2} benchmarked by $\epsilon_{V_1,8}$, i.e. $\epsilon_{V_1,8}/\epsilon_{V_{\text{mix},K_1,K_2}}$. Observe that the cost decreases linearly with p , while the achieved error does not drop significantly until $p > 0.8$. RTS thus can achieve much higher accuracy with certain a gate cost. For example, at $p \approx 0.85$, the cost for $V_{\text{m},7,10}$ and $V_{\text{m},7,11}$ are roughly the same as implementing $V_{1,8}$, but the accuracies achieved are $96\times$ and $472\times$ better respectively. Note that both of the examples here are not optimal.

Conclusion.— We presented a simple framework RTS that applies to all quantum algorithms relying on truncated series approximation. RTS enables a “fractional” truncation order and provides a quadratic improvement on truncation error. Essentially, we developed a random mixing protocol with two input quantum circuits V_1 and V_2 . Their truncation errors cancel out each other during

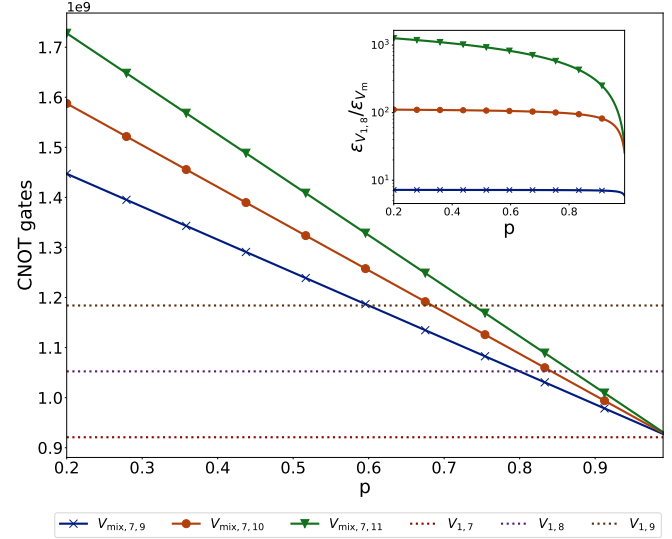


FIG. 2. Relationship between CNOT gate cost and p . V_{mix,K_1,K_2} is the quantum circuit created by RTS with $V_{1(2)}$ truncated at $K_{1(2)}$. The cost for V_{m,K_1,K_2} linearly decreases with increasing p . The subgraph shows the multiplicative accuracy improvement. $\epsilon_{V_1,8}$ is the error obtained by $V_{1,8}$, and we divided by $\epsilon_{V_{\text{m},K_1,K_2}}$, which are error corresponds to three V_{m,K_1,K_2} .

the mixing channel, and with the newly introduced mixing probability p , continuous adjustment of the overall cost (equivalently truncation order) becomes viable. We specifically exhibit the implementation of RTS in the context of Hamiltonian Simulation, Uniform Spectral Amplification, and Solving time-independent ODE. These illustrate the flexibility of RTS to be embedded in other algorithms as presented in ODE implementation, and to encompass subroutines like Oblivious Amplitude Amplification and the linear combination of multiple polynomials. Finally, we simulate the reduction of the CNOT gate in the BCCKS algorithm.

We note that RTS can also apply to the recently proposed LCHS [43, 44] and QEP [45] algorithms simulating non-unitary dynamics. Although no integer constraint applies truncated-integral algorithms like LCHS, employing RTS also offers a quadratic improvement on truncation error. We anticipate the generalization of the framework into dynamics determined by time-dependent operators, i.e. Dyson series, and analog quantum computing model.

ACKNOWLEDGMENTS

We thank Andrew Childs, Xiao Yuan, Xiongfeng Ma, and You Zhou for their helpful discussion and suggestions. We acknowledge the funding from HKU Seed Fund for Basic. We acknowledge funding from HKU Seed Fund for Basic Research for New Staff via Project 2201100596, Guangdong Natural Science Fund—General Programme

via Project 2023A1515012185, National Natural Science Foundation of China (NSFC) Young Scientists Fund via Project 12305030, Hong Kong Research Grant Council (RGC) via No. 27300823, and NSFC/RGC Joint Research Scheme via Project N_HKU718/23.

REFERENCES

- [1] S. Lloyd, Universal quantum simulators, *Science* **273**, 1073 (1996).
- [2] G. H. Low and I. L. Chuang, Hamiltonian Simulation by Qubitization, *Quantum* **3**, 163 (2019).
- [3] G. H. Low, *Quantum Signal Processing by Single-Qubit Dynamics*, Thesis, Massachusetts Institute of Technology (2017).
- [4] D. W. Berry, A. M. Childs, R. Cleve, R. Kothari, and R. D. Somma, Simulating Hamiltonian Dynamics with a Truncated Taylor Series, *Physical Review Letters* **114**, 090502 (2015).
- [5] A. M. Childs, A. Ostrander, and Y. Su, Faster quantum simulation by randomization, *Quantum* **3**, 182 (2019).
- [6] A. M. Childs and Y. Su, Nearly optimal lattice simulation by product formulas, *Phys. Rev. Lett.* **123**, 050503 (2019).
- [7] Q. Zhao, Y. Zhou, A. F. Shaw, T. Li, and A. M. Childs, Hamiltonian simulation with random inputs, *Phys. Rev. Lett.* **129**, 270502 (2022).
- [8] D. W. Berry, A. M. Childs, A. Ostrander, and G. Wang, Quantum algorithm for linear differential equations with exponentially improved dependence on precision, *Communications in Mathematical Physics* **356**, 1057 (2017), arxiv:1701.03684 [quant-ph].
- [9] H. Krovi, Improved quantum algorithms for linear and nonlinear differential equations, *Quantum* **7**, 913 (2023), arxiv:2202.01054 [physics, physics:quant-ph].
- [10] A. Gilyén, Y. Su, G. H. Low, and N. Wiebe, Quantum singular value transformation and beyond: Exponential improvements for quantum matrix arithmetics, in *Proceedings of the 51st Annual ACM SIGACT Symposium on Theory of Computing* (2019) pp. 193–204, arxiv:1806.01838 [quant-ph].
- [11] C. Sünderhauf, Generalized quantum singular value transformation (2023), arXiv:2312.00723 [quant-ph].
- [12] J. M. Martyn, Z. M. Rossi, A. K. Tan, and I. L. Chuang, A Grand Unification of Quantum Algorithms, *PRX Quantum* **2**, 040203 (2021), arxiv:2105.02859 [quant-ph].
- [13] D. A. Lidar and H. Wang, Calculating the thermal rate constant with exponential speedup on a quantum computer, *Phys. Rev. E* **59**, 2429 (1999).
- [14] G. Ortiz, J. E. Gubernatis, E. Knill, and R. Laflamme, Quantum algorithms for fermionic simulations, *Phys. Rev. A* **64**, 022319 (2001).
- [15] D. Wecker, B. Bauer, B. K. Clark, M. B. Hastings, and M. Troyer, Gate-count estimates for performing quantum chemistry on small quantum computers, *Physical Review A* **90**, 022305 (2014).
- [16] R. Babbush, C. Gidney, D. W. Berry, N. Wiebe, J. McClean, A. Paler, A. Fowler, and H. Neven, Encoding Electronic Spectra in Quantum Circuits with Linear T Complexity, *Physical Review X* **8**, 041015 (2018).
- [17] R. Babbush, N. Wiebe, J. McClean, J. McClain, H. Neven, and G. K.-L. Chan, Low Depth Quantum Simulation of Electronic Structure, *Physical Review X* **8**, 011044 (2018), arxiv:1706.00023 [physics, physics:quant-ph].
- [18] S. McArdle, S. Endo, A. Aspuru-Guzik, S. C. Benjamin, and X. Yuan, Quantum computational chemistry, *Rev. Mod. Phys.* **92**, 015003 (2020).
- [19] P. C. S. Costa, S. Jordan, and A. Ostrander, Quantum algorithm for simulating the wave equation, *Physical Review A* **99**, 012323 (2019).
- [20] J. Haah, M. B. Hastings, R. Kothari, and G. H. Low, Quantum algorithm for simulating real time evolution of lattice Hamiltonians, *SIAM Journal on Computing* **52**, FOCS18 (2023), arxiv:1801.03922 [quant-ph].
- [21] K. Mizuta and K. Fujii, Optimal Hamiltonian simulation for time-periodic systems, *Quantum* **7**, 962 (2023), arxiv:2209.05048 [cond-mat, physics:quant-ph].
- [22] P. W. Shor, Polynomial-Time Algorithms for Prime Factorization and Discrete Logarithms on a Quantum Computer, *SIAM Journal on Computing* **26**, 1484 (1997), arxiv:quant-ph/9508027.
- [23] X. Li, X. Yin, N. Wiebe, J. Chun, G. K. Schenter, M. S. Cheung, and J. Mülmenstädt, *Potential quantum advantage for simulation of fluid dynamics* (2023), arxiv:2303.16550 [physics, physics:quant-ph].
- [24] A. Ameri, E. Ye, P. Cappellaro, H. Krovi, and N. F. Loureiro, Quantum algorithm for the linear Vlasov equation with collisions, *Physical Review A* **107**, 062412 (2023).
- [25] N. Linden, A. Montanaro, and C. Shao, Quantum vs. Classical Algorithms for Solving the Heat Equation, *Communications in Mathematical Physics* **395**, 601 (2022).
- [26] D. Herman, C. Googin, X. Liu, A. Galda, I. Safro, Y. Sun, M. Pistoia, and Y. Alexeev, A Survey of Quantum Computing for Finance (2022), arxiv:2201.02773 [quant-ph, q-fin].
- [27] D. Stilck França and R. Garcia-Patron, Limitations of optimization algorithms on noisy quantum devices, *Nature Physics* **17**, 1221 (2021).
- [28] Y. Zhou, E. M. Stoudenmire, and X. Waintal, What Limits the Simulation of Quantum Computers?, *Physical Review X* **10**, 041038 (2020).
- [29] Y. Kikuchi, C. Mc Keever, L. Coopmans, M. Lubasch, and M. Benedetti, Realization of quantum signal processing on a noisy quantum computer, *npj Quantum Information* **9**, 1 (2023).
- [30] R. Meister, S. C. Benjamin, and E. T. Campbell, Tailoring Term Truncations for Electronic Structure Calculations Using a Linear Combination of Unitaries, *Quantum* **6**, 637 (2022).
- [31] Q. Zhao and X. Yuan, Exploiting anticommutation in Hamiltonian simulation, *Quantum* **5**, 534 (2021).
- [32] M. Reiher, N. Wiebe, K. M. Svore, D. Wecker, and M. Troyer, Elucidating reaction mechanisms on quantum computers, *Proceedings of the National Academy of Sciences* **114**, 7555 (2017).
- [33] A. M. Childs, D. Maslov, Y. Nam, N. J. Ross, and Y. Su, Toward the first quantum simulation with quantum speedup, *Proceedings of the National Academy of Sciences* **115**, 9456 (2018).
- [34] E. Campbell, Shorter gate sequences for quantum computing by mixing unitaries, *Physical Review A* **95**, 042306 (2017).
- [35] M. B. Hastings, Turning Gate Synthesis Errors into

Incoherent Errors, <https://arxiv.org/abs/1612.01011v1> (2016).

[36] Kothari, Robin, *Efficient algorithms in quantum query complexity*, Ph.D. thesis, University of Waterloo (2014).

[37] D. W. Berry, A. M. Childs, R. Cleve, R. Kothari, and R. D. Somma, Exponential improvement in precision for simulating sparse Hamiltonians, in *Proceedings of the Forty-Sixth Annual ACM Symposium on Theory of Computing* (2014) pp. 283–292, [arxiv:1312.1414](https://arxiv.org/abs/1312.1414) [quant-ph].

[38] M. Abramowitz, I. A. Stegun, and R. H. Romer, Handbook of mathematical functions with formulas, graphs, and mathematical tables (1988).

[39] D. Nagaj, P. Wocjan, and Y. Zhang, Fast amplification of qma (2009), [arXiv:0904.1549](https://arxiv.org/abs/0904.1549) [quant-ph].

[40] R. D. Somma and S. Boixo, Spectral gap amplification, *SIAM Journal on Computing* **42**, 593 (2013), <https://doi.org/10.1137/120871997>.

[41] D. W. Berry, High-order quantum algorithm for solving linear differential equations, *Journal of Physics A: Mathematical and Theoretical* **47**, 105301 (2014), [arxiv:1010.2745](https://arxiv.org/abs/1010.2745) [quant-ph].

[42] J.-P. Liu and L. Lin, Dense outputs from quantum simulations (2023), [arxiv:2307.14441](https://arxiv.org/abs/2307.14441) [quant-ph].

[43] D. An, J.-P. Liu, and L. Lin, Linear Combination of Hamiltonian Simulation for Nonunitary Dynamics with Optimal State Preparation Cost, *Physical Review Letters* **131**, 150603 (2023).

[44] D. An, A. M. Childs, and L. Lin, Quantum algorithm for linear non-unitary dynamics with near-optimal dependence on all parameters, arXiv preprint [arXiv:2312.03916](https://arxiv.org/abs/2312.03916) (2023).

[45] G. H. Low and Y. Su, Quantum eigenvalue processing (2024), [arxiv:2401.06240](https://arxiv.org/abs/2401.06240) [physics, physics:quant-ph].

[46] A. M. Childs and N. Wiebe, Hamiltonian Simulation Using Linear Combinations of Unitary Operations, *Quantum Information and Computation* **12**, 10.26421/QIC12.11-12 (2012), [arxiv:1202.5822](https://arxiv.org/abs/1202.5822) [quant-ph].

[47] A. M. Childs, R. Kothari, and R. D. Somma, Quantum algorithm for systems of linear equations with exponentially improved dependence on precision, *SIAM Journal on Computing* **46**, 1920 (2017), [arxiv:1511.02306](https://arxiv.org/abs/1511.02306) [quant-ph].

Appendix A: Proof of Lemma 1

Proof. From the assumption of operator norm, we have

$$\|V_1|\psi\rangle - U|\psi\rangle\|_1 \leq a_1, \quad \|V_2|\psi\rangle - U|\psi\rangle\|_1 \leq a_2, \quad \|V_m|\psi\rangle - U|\psi\rangle\|_1 \leq b \quad (\text{A1})$$

We denote the non-normalized state $\mathcal{V}_{mix}(\rho) = pV_1|\psi\rangle\langle\psi|V_1^\dagger + (1-p)V_2|\psi\rangle\langle\psi|V_2^\dagger$, $|\epsilon_1\rangle = V_1|\psi\rangle - U_0|\psi\rangle$, $|\epsilon_2\rangle = V_2|\psi\rangle - U_0|\psi\rangle$, and $|\epsilon_m\rangle = (pV_1 + (1-p)V_2)|\psi\rangle - U_0|\psi\rangle = p|\epsilon_1\rangle + (1-p)|\epsilon_2\rangle$.

$$\begin{aligned} \rho - U_0|\psi\rangle\langle\psi|U_0^\dagger &= p(U_0|\psi\rangle + |\epsilon_1\rangle)(\langle\epsilon_1| + \langle\psi|U_0^\dagger) + (1-p)(U_0|\psi\rangle + |\epsilon_2\rangle)(\langle\epsilon_2| + \langle\psi|U_0^\dagger) - U_0|\psi\rangle\langle\psi|U_0^\dagger \\ &= |\epsilon_m\rangle\langle\psi|U_0^\dagger + U_0|\psi\rangle\langle\epsilon_m| + p|\epsilon_1\rangle\langle\epsilon_1| + (1-p)|\epsilon_1\rangle\langle\epsilon_1|. \end{aligned} \quad (\text{A2})$$

According to the definitions, $\|\epsilon_1\| \leq a_1$, $\|\epsilon_2\| \leq a_2$, $\|\epsilon_m\| = \sqrt{\langle\epsilon_m|\epsilon_m\rangle} \leq b$,

$$\begin{aligned} \|\rho - U_0|\psi\rangle\langle\psi|U_0^\dagger\|_1 &\leq \|\epsilon_m\|\langle\psi|U_0^\dagger\|_1 + \|U_0|\psi\rangle\langle\epsilon_m\|_1 + p\|\epsilon_1\|\langle\epsilon_1\|_1 + (1-p)\|\epsilon_2\|\langle\epsilon_2\|_1 \\ &\leq 2\sqrt{\langle\epsilon_m|\epsilon_m\rangle} + p\langle\epsilon_1|\epsilon_1\rangle + (1-p)\langle\epsilon_2|\epsilon_2\rangle \\ &\leq 2b + pa_1^2 + (1-p)a_2^2 = \varepsilon. \end{aligned} \quad (\text{A3})$$

This also implies $1 - \varepsilon \leq \|\rho\|_1 \leq 1 + \varepsilon$

$$\left\| \frac{\rho}{\|\rho\|_1} - U_0|\psi\rangle\langle\psi|U_0^\dagger \right\|_1 \leq \left\| \rho - U_0|\psi\rangle\langle\psi|U_0^\dagger \right\|_1 + \|\rho\|_1 \left(\frac{1}{\|\rho\|_1} - 1 \right) \leq 2\varepsilon. \quad (\text{A4})$$

□

Appendix B: Framework implementation on BCCKS algorithm

In the BCCKS algorithm, we tried to expand the unitary, $U = e^{-iHt}$, through a truncated Taylor's series, where each term can be represented by products of unitaries. We then apply the LCU algorithm [46] to put these unitaries together to approximate U .

Note any Hamiltonian H can be represented by a sum of unitary components, i.e.

$$H = \sum_{l=1}^L \alpha_l H_l. \quad (\text{B1})$$

We truncate the Taylor's series at order K and approximate U by

$$\tilde{U} := \sum_{k=0}^K \frac{1}{k!} (-iHt)^k = \sum_{k=0}^K \sum_{l_1, \dots, l_k=1}^L \underbrace{\frac{\alpha_{l_1}\alpha_{l_2}\dots\alpha_{l_k}t^k}{k!}}_{\text{Coefficients}} \underbrace{(-i)^k H_{l_1}H_{l_2}\dots H_{l_k}}_{\text{Unitaries}}, \quad (\text{B2})$$

where each $\alpha_l \geq 0$ since we can absorb the negative sign in H_l . \tilde{U} is in a standard form of LCU, i.e. $\sum_j \beta_j \tilde{V}_j$ for coefficients β_j and unitaries \tilde{V}_j :

To implement the LCU algorithm, we first define two oracles

$$\begin{aligned} G|0\rangle &:= \frac{1}{\sqrt{s}} \sum_j \sqrt{\beta_j} |j\rangle \\ \text{select}(\tilde{U}) &:= \sum_j |j\rangle\langle j| \otimes \tilde{V}_j, \end{aligned} \quad (\text{B3})$$

where $s = \sum_{j=0}^{L^K-1} \beta_j$.

With these two oracle, we can construct

$$W := (G^\dagger \otimes \mathbb{1}) \text{select}(\tilde{U}) (G \otimes \mathbb{1}), \quad (\text{B4})$$

where $\mathbb{1}$ is the identity operator. Such that

$$PW|0\rangle|\psi\rangle = \frac{1}{s}|0\rangle\tilde{U}|\psi\rangle + |\perp\rangle, \quad (\text{B5})$$

where $P := |0\rangle\langle 0| \otimes \mathbb{1}$ and $(\langle 0| \otimes \mathbb{1})|\perp\rangle = 0$.

Therefore, we probabilistically obtain $\tilde{U}|\psi\rangle$. Applying oblivious amplitude amplification (OAA) [37] amplifies the success probability to near unity. Practically, the t is very large and s scales with t . We, therefore, have to divide t into r segments with each segment corresponding to an evolution time of $\tau = t/r = \ln 2/(\sum_{l=1}^L \alpha_l)$ such that each segment has $s = 2$ in the case of $K = \infty$. Although this means $s < 2$ in the actual algorithm, OAA is robust as long as $|s - 2| \leq \mathcal{O}(\epsilon)$ and $\|\tilde{U} - U\| \leq \mathcal{O}(\epsilon)$ as analysed in ref. [4]. Consecutively applying this segment r times gives the final Hamiltonian simulation. The last segment has time smaller than τ , and its treatment is illustrated in ref. [37] with the cost of one additional ancillary qubit. In the following discussion, we assume the evolution time to be τ , and the error and cost corresponding to evolution time t can be retrieved by multiplying r .

Finally, we have

$$PTW(|0\rangle \otimes |\Psi\rangle) = |0\rangle \otimes \left(\frac{3}{s}\tilde{U} - \frac{4}{s^3}\tilde{U}\tilde{U}^\dagger\tilde{U} \right) |\Psi\rangle, \quad (\text{B6})$$

where $T = -WRW^\dagger R$, and $R = (\mathbb{1} - 2|0\rangle\langle 0|) \otimes \mathbb{1}$.

We use $V_1 := (\langle 0| \otimes \mathbb{1})PTW(|0\rangle \otimes \mathbb{1})$ to approximate a K_1 truncation. Additionally, we define the index set J_1 for the mapping from $j \in J_1$ index to the tuple $(k, l_1, l_2, \dots, l_k)$ as

$$J_1 := \{(k, l_1, l_2, \dots, l_k) : k \in \mathbb{N}, k \leq K_1, l_1, l_2, \dots, l_k \in \{1, \dots, L\}\}. \quad (\text{B7})$$

We can then write F_1 in the standard form of LCU

$$\begin{aligned} F_1 &= \sum_{k=0}^{K_1} \frac{1}{k!} (-iH\tau)^k \\ &= \sum_{k=0}^{K_1} \sum_{l_1, \dots, l_k=1}^L \frac{\alpha_{l_1}\alpha_{l_2}\dots\alpha_{l_k}t^k}{k!} (-i)^k H_{l_1}H_{l_2}\dots H_{l_k} \\ &= \sum_{j \in J_1} \beta_j \tilde{V}_j. \end{aligned} \quad (\text{B8})$$

Thus, F_1 can be implemented by invoking G_1 and select(F_1) with the same definition in Eq. (B3) with $j \in J_1$.

Lemma 2. (Error and success probability of V_1)

The quantum circuit V_1 implements F_1 , approximating the unitary $U = e^{-iH\tau}$ with error bounded by

$$\begin{aligned} \|V_1 - U\| &\leq a_1 \\ a_1 &= \delta_1 \left(\frac{\delta_1^2 + 3\delta_1 + 4}{2} \right), \end{aligned} \quad (\text{B9})$$

where $\delta_1 = 2 \frac{(\ln 2)^{K_1+1}}{(K_1+1)!}$. The success probability is lower bounded by $\theta_1 \geq (1 - a_1)^2$.

Proof. We can bound the truncation error of F_1 by

$$\begin{aligned} \|F_1 - U\| &= \left\| \sum_{k=K_1+1}^{\infty} \frac{(-iH\tau)^k}{k!} \right\| \\ &\leq \sum_{k=K_1+1}^{\infty} \frac{(\|H\|t)^k}{k!} \\ &\leq \sum_{k=K_1+1}^{\infty} \frac{\left(\tau \sum_{l=1}^L \alpha_l\right)^k}{k!} \\ &= \sum_{k=K_1+1}^{\infty} \frac{(\ln 2)^k}{k!} \\ &\leq 2 \frac{(\ln 2)^{K_1+1}}{(K_1+1)!} =: \delta_1. \end{aligned} \quad (\text{B10})$$

Therefore, the following holds,

$$\|F_1\| \leq \|F_1 - U\| + \|U\| \leq 1 + \delta_1 \quad (\text{B11})$$

and

$$\begin{aligned} \|F_1 F_1^\dagger - \mathbb{1}\| &\leq \|F_1 F_1^\dagger - UF_1^\dagger\| + \|UF_1^\dagger - UU^\dagger\| \\ &\leq \delta_1 (1 + \delta_1) + \delta_1 = \delta_1 (2 + \delta_1). \end{aligned} \quad (\text{B12})$$

Eventually, we complete the proof of error bound by

$$\begin{aligned} \|V_1 - U\| &= \left\| \frac{3}{2}F_1 - \frac{1}{2}F_1 F_1^\dagger F_1 - U \right\| \\ &\leq \|F_1 - U\| + \frac{1}{2} \|F_1 - F_1 F_1^\dagger F_1\| \\ &\leq \delta_1 + \frac{\delta_1(1 + \delta_1)(2 + \delta_1)}{2} = \delta_1 \left(\frac{\delta_1^2 + 3\delta_1 + 4}{2} \right) = a_1. \end{aligned} \quad (\text{B13})$$

As for the success probability, we apply lemma G.4. in ref. [33] to claim that it is greater than $(1 - a_1)^2$ \square

The other quantum circuit V_2 implements the sum

$$\begin{aligned} F_2 &= \sum_{k=0}^{K_1} \frac{1}{k!} (-iH\tau)^k + \frac{1}{1-p} \sum_{k=K_1+1}^{K_2} \frac{1}{k!} (-iH\tau)^k \\ &= \sum_{k=0}^{K_1} \sum_{l_1, \dots, l_k=1}^L \frac{\alpha_{l_1} \alpha_{l_2} \dots \alpha_{l_k} t^k}{k!} (-i)^k H_{l_1} H_{l_2} \dots H_{l_k} + \frac{1}{1-p} \sum_{k=K_1+1}^{K_2} \sum_{l_1, \dots, l_k=1}^L \frac{\alpha_{l_1} \alpha_{l_2} \dots \alpha_{l_k} t^k}{k!} (-i)^k H_{l_1} H_{l_2} \dots H_{l_k} \\ &= \sum_{j \in J_2} \beta_j \tilde{V}_j, \end{aligned} \quad (\text{B14})$$

Where $J_2 := \{(k, l_1, l_2, \dots, l_k) : k \in \mathbb{N}, k \leq K_2, l_1, l_2, \dots, l_k \in \{1, \dots, L\}\}$. Since we already set $\tau \sum_{l=1}^L \alpha_l = \ln 2$, and we must have $2p\delta_1/(1-p) \leq a_2$ holds for bounding error in OAA, which can be easily violated as we increase p . We, hence, amplify $s_2 = \sum_{j \in J_2} \beta_j$ to $\sin^{-1}(\pi/10)$, and we will need one more flip to achieve approximately unit success probability. We also define G_2 and select(F_2) as in Eq. (B3) with $j \in J_2$.

Lemma 3. (Error and success probability of V_2)

The quantum circuit V_2 implements F_2 , approximating the unitary $U = e^{-iH\tau}$ with error bounded by

$$\begin{aligned} \|V_2 - U_0\| &\leq a_2 \\ a_2 &= \left(1 + \frac{40}{s_2^3} + \frac{64}{s_2^5} \right) \delta_2, \end{aligned} \quad (\text{B15})$$

where $\delta_2 = \frac{p}{1-p} \frac{(\ln 2)^{K_1+1}}{(K_1+1)!}$ and $s_2 = \sin^{-1}(\pi/10)$. The success probability is lower bounded by $\theta_2 \geq (1 - a_2)^2$.

Proof. The operator we are approximating using V_2 is

$$F_2 = \sum_{k=0}^{K_1} \frac{(-iHt)^k}{k!} + \frac{1}{1-p} \sum_{k=K_1+1}^{K_2} \frac{(-iHt)^k}{k!}. \quad (\text{B16})$$

With another set of oracles as Eq. (B3), G_2 preparing the coefficients and select(V)₂ applying unitaries for Eq. (B16), we can construct $W_2 = (G_2^\dagger \otimes \mathbb{1}) \text{select}(F_2)(G_2 \otimes \mathbb{1})$, such that

$$W_2(|0\rangle \otimes |\psi\rangle) = \frac{1}{s'_2} (|0\rangle \otimes F_2 |\psi\rangle) + |\perp\rangle, \quad (\text{B17})$$

where $(\langle 0 | \otimes \mathbb{1}) |\perp\rangle = 0$ and we can approximate s'_2 by

$$s'_2 = \sum_{k=0}^{K_1} \frac{\left(\tau \sum_{l=1}^L \alpha_l \right)^k}{k!} + \frac{1}{1-p} \sum_{k=K_1+1}^{K_2} \frac{\left(\tau \sum_{l=1}^L \alpha_l \right)^k}{k!} \approx \exp(\ln 2) + \frac{p(\ln 2)^{K_1+1}}{(1-p)(K_1+1)!} \exp(\ln 2) = 2 + \frac{2p}{(1-p)} \delta_1. \quad (\text{B18})$$

We want to amplify $1/s'_2$ to 1 by applying OAA. Although s'_2 is unbounded above when $p \rightarrow 1$, $\{K_1, K_2, p\}$ with extreme p will be discarded when transversing viable sets for a given cost budget. Therefore, it is safe for us to bound $p \leq 1/(1+2\delta_1)$ such that $s'_2 \leq 3$ and we can always amplify s'_2 to $s_2 = \sin^{-1}(\pi/10)$.

We can perform *PTTW* to approach certainty, such that

$$PTTW(|0\rangle \otimes |\psi\rangle) = |0\rangle \otimes \left(\frac{5}{s_2} F_2 - \frac{20}{s_2^3} F_2 F_2^\dagger F_2 + \frac{16}{s_2^5} F_2 F_2^\dagger F_2 F_2^\dagger F_2 \right) |\psi\rangle. \quad (\text{B19})$$

Therefore, we have the unitary

$$\begin{aligned} V_2 &= (\langle 0 | \otimes \mathbb{1}) PTTW(|0\rangle \otimes \mathbb{1}) \\ &= \left(\frac{5}{s_2} - \frac{20}{s_2^3} + \frac{16}{s_2^5} \right) F_2 - \frac{20}{s_2^3} (F_2 F_2^\dagger F_2 - F_2) + \frac{16}{s_2^5} (F_2 F_2^\dagger F_2 F_2^\dagger F_2 - F_2). \end{aligned} \quad (\text{B20})$$

We denote the truncated error in F_2 as δ_2 , where

$$\delta_2 = \left| -\frac{p}{1-p} \frac{(\ln 2)^{K_1+1}}{(K_1+1)!} + \frac{2}{1-p} \frac{(\ln 2)^{K_2+1}}{(K_2+1)!} \right| \leq \frac{p}{1-p} \frac{(\ln 2)^{K_1+1}}{(K_1+1)!} = \frac{p}{1-p} \delta_1 \quad (\text{B21})$$

With the facts $\|F_2\| \leq 1 + \delta_2$, $\|F_2^\dagger F_2 - I\| \leq \delta_2(2 + \delta_2)$, and

$$\begin{aligned} \|F_2^\dagger F_2 F_2^\dagger F_2 - \mathbb{1}\| &\leq \|F_2^\dagger F_2 F_2^\dagger F_2 - F_2^\dagger F_2\| + \|F_2^\dagger F_2 - \mathbb{1}\| \\ &\leq \|F_2^\dagger F_2\| \delta_2(2 + \delta_2) + \delta_2(2 + \delta_2) \\ &\leq [(1 + \delta_2)^2 + 1] \delta_2(2 + \delta_2) = \delta_2(2 + \delta_2)(2 + 2\delta_2 + \delta_2^2) \\ &\approx 4\delta_2. \end{aligned} \quad (\text{B22})$$

We can thereby compute $\|V_2\|$ terms by terms. In the first term in the last line of equation ((B20)), we have

$$\frac{5}{s_2} - \frac{20}{s_2^3} + \frac{16}{s_2^5} \leq 1. \quad (\text{B23})$$

For the rest,

$$\begin{aligned} \left\| \frac{20}{s_2^3} (F_2 F_2^\dagger F_2 - F_2) \right\| &\leq \frac{20}{s_2^3} (1 + \delta_2) \delta_2 (2 + \delta_2) \leq \frac{80}{s_2^3} \delta_2 \\ \left\| \frac{16}{s_2^5} (F_2 F_2^\dagger F_2 F_2^\dagger F_2 - F_2) \right\| &\leq \frac{16}{s_2^5} (1 + \delta_2) \delta_2 (2 + \delta_2) (2 + 2\delta_2 + \delta_2^2) \leq \frac{128}{s_2^5} \delta_2. \end{aligned} \quad (\text{B24})$$

Consequently,

$$\|V_2 - U_0\| \leq \left(1 + \frac{80}{s_2^3} + \frac{128}{s_2^5} \right) \delta_2 \leq 4\delta_2 = a_2. \quad (\text{B25})$$

The success probability follows similarly to be greater than $(1 - a_2)^2$ \square

The last ingredient is the calculation of the error bound on $V_m = pV_1 + (1-p)V_2$.

Lemma 4. (*Error of V_m*)

The quantum circuit V_m implemented by mixing two quantum circuits V_1 and V_2 with probability p and $1-p$ respectively approximates $U = e^{-iH\tau}$ with bounded error

$$\begin{aligned} \|V_m - U\| &\leq b \\ b &= \delta_m + \frac{9p - 6p^2}{(1-p)^2} a_1^2, \end{aligned} \quad (\text{B26})$$

where $\delta_m = 2 \frac{(\ln 2)^{K_2+1}}{(K_2+1)!}$.

Proof. We cannot trivially add each term in F_1 and F_2 linearly because each of V_1 and V_2 is reflected during OAA. We, therefore, give a loose upper bound by analyzing each term in the error sources separately.

Observe that we have $U = F_1 + E_1$ and $U = F_2 + E_2$, where E_1 and E_2 are truncation errors with,

$$\begin{aligned} E_1 &= \sum_{k=K_1+1}^{\infty} (-iH\tau)^k, \\ E_2 &= -\frac{p}{1-p} \sum_{k=K_1+1}^{K_2} (-iH\tau) + \sum_{k=K_2}^{\infty} (-iH\tau)^k, \end{aligned} \tag{B27}$$

and we can bound their absolute value by δ_1 and δ_2 respectively. We can thus express

$$\begin{aligned} V_1 &= U + \frac{1}{2}(E_1 - U^\dagger E_1 U) + R_1 \\ V_2 &= U + \frac{1}{2}(E_2 - U^\dagger E_2 U) + R_2, \end{aligned} \tag{B28}$$

where $\|R_1\| \leq \frac{3}{2}\|E_1\|^2 + \frac{1}{2}\|E_1\|^3 \leq \frac{3}{2}\delta_1^2 + \frac{1}{2}\delta_1^3$ and $\|R_2\| \leq (\frac{80}{s^3} + \frac{128}{s^5})\|E_2\|^2 + \mathcal{O}(\|E_2\|^3) \leq \frac{3p^2}{(1-p)^2}\delta_1^2$ are the truncation error after OAA. These bounds can be derived after invoking lemma 2 and 3.

Lastly, note that

$$\|pE_1 + (1-p)E_2\| = \left\| \sum_{k=K_2}^{\infty} (-iH\tau)^k \right\| \leq 2 \frac{(\ln 2)^{K_2+1}}{(K_2+1)!} =: \delta_m, \tag{B29}$$

combining equation ((B28)) and ((B29)), we have

$$\begin{aligned} \|pV_1 + (1-p)V_2 - U\| &= \left\| \frac{1}{2}[(pE_1 + (1-p)E_2) - U_0^\dagger(pE_1 + (1-p)E_2)U_0] + pR_1 + (1-p)R_2 \right\| \\ &\leq \delta_m + p \left(\frac{3}{2}\delta_1^2 + \frac{1}{2}\delta_1^3 \right) + (1-p) \left(\frac{3p^2}{(1-p)^2}\delta_1^2 \right) \\ &\leq \delta_m + \frac{3}{1-p}\delta_1^2 + \mathcal{O}(\delta_1^3) =: b, \end{aligned} \tag{B30}$$

where the inequality in second line holds because an operator O satisfy $\|O\| \leq \|U^\dagger OU\|$ for any unitary U □

Proof of Theorem 1

Proof. From lemma 1, we know the error after mixing channel can be expressed by a_1 a_2 and b , which were derived in lemma 2, 3 and 4. We can combine the results to get

$$\begin{aligned} \epsilon &= 4b + 2pa_1^2 + 2(1-p)a_2^2 \\ &= 4 \left(\delta_m + \frac{3}{1-p}\delta_1^2 + \mathcal{O}(\delta_1^3) \right) + 2(1-p) \left(1 + \frac{80}{s_2^3} + \frac{128}{s_2^5} \right)^2 \delta_2^2 + 2p \left(\delta_1 \left(\frac{\delta_1^2 + 3\delta_1 + 4}{2} \right) \right)^2 \\ &\leq \frac{20}{1-p}\delta_1^2 + 4\delta_m \\ &\leq \max \left\{ \frac{40}{1-p}\delta_1^2, 8\delta_m \right\}, \end{aligned} \tag{B31}$$

where the equality in the last line holds because δ_m is exponentially smaller than δ_1 . As for the success probability, according to [33], the lower bound on success probability for each of implementing V_1 and V_2 are $(1-a_1)^2$ and $(1-a_2)^2$ respectively. Therefore, the overall algorithm success with the probability of at least

$$\begin{aligned} \theta &\geq p(1-a_1)^2 + (1-p)(1-a_2)^2 \\ &\geq 1 - \frac{8}{1-p}\delta_1^2 + \delta_1^2 - 4\delta_1. \end{aligned} \tag{B32}$$

It implies that the failure probability $\xi \leq \frac{8}{1-p}\delta_1^2 + 4\delta_1$. □

Appendix C: QSP

QSP equips us with the tool for implementing non-linear combinations of Hamiltonians H , i.e. $f[H]$ subject to some constraints. In this section, we will analyze how to apply RTS to two instances in QSP, namely Hamiltonian Simulation and Uniform Spectral Amplification(USA). Oracles in QSP are similar to what was discussed in LCU. However, we express them in another form to be consistent with existing literature [2, 3, 46]. Note that all variables in this section are irreverent to definitions in the last section.

Assuming we have two oracles with \hat{G} prepares the state

$$\hat{G} |0\rangle_a = |G\rangle_a \in \mathcal{H}_a, \quad (\text{C1})$$

in the ancillary space \mathcal{H}_a and \hat{U} block encodes the Hamiltonian H such that

$$\begin{aligned} \hat{U} |G\rangle_a |\lambda\rangle_s &= |G\rangle_a H |\lambda\rangle_s + \sqrt{1 - \|H|\lambda\rangle\|^2} |G^\perp\rangle_a |\lambda\rangle_s \\ &= \lambda |G_\lambda\rangle_{as} + \sqrt{1 - |\lambda|^2} |G_\lambda^\perp\rangle_{as} \end{aligned} \quad (\text{C2})$$

where $|\lambda\rangle_s$ is one of the eigenstates of H in the subspace \mathcal{H}_s and λ is the corresponding eigenvalue such that $H|\lambda\rangle_s = \lambda|\lambda\rangle_s$, $|G_\lambda\rangle_{as}$ is the abbreviation of $|G\rangle_a |\lambda\rangle_s$ and $(\langle G|_a \otimes \hat{1}) |G_\lambda^\perp\rangle_{as} = 0$. However, successively applying \hat{U} does not produce powers of λ . Because its action on $|G_\lambda^\perp\rangle_{as}$ contaminates the block we are interested in. We thus need to construct a unitary iterate \hat{W}

$$\begin{aligned} \hat{W} &= ((2|G\rangle\langle G| - \hat{1}_a) \otimes \hat{1}_s) \hat{S} \hat{U} \\ &= \begin{pmatrix} \lambda |G_\lambda\rangle\langle G_\lambda| & -\sqrt{1 - |\lambda|^2} |G_\lambda\rangle\langle G_\lambda^\perp| \\ \sqrt{1 - |\lambda|^2} |G_\lambda^\perp\rangle\langle G_\lambda| & \lambda |G_\lambda^\perp\rangle\langle G_\lambda^\perp| \end{pmatrix}, \end{aligned} \quad (\text{C3})$$

where the construction of \hat{S} is out of the scope of this article, and details can be found in ref. [2]. Note that from lemma 17 in ref. [47]

$$\hat{W}^n = \begin{pmatrix} \mathcal{T}_n(\lambda) & \cdot \\ \cdot & \cdot \end{pmatrix}, \quad (\text{C4})$$

where $\mathcal{T}_n(\lambda)$ is the n -th order Chebyshev polynomial. However, $f[H]$ available for \hat{W} is limited due to the restriction on parity. We can add an ancilla in subspace \mathcal{H}_b to rotate \hat{W} for a wider variety of $f[H]$. Define $\hat{V} = e^{i\Phi} \hat{W}$, $\hat{V}_0 = |+\rangle\langle +|_b \otimes \hat{1}_s + |-\rangle\langle -|_b \otimes \hat{V}$, and

$$\hat{V}_{\vec{\varphi}} = \prod_{\text{odd } k=1}^{K/2} \hat{V}_{\varphi_{k+1} + \pi}^\dagger \hat{V}_{\varphi_k}, \quad (\text{C5})$$

where $\hat{V}_\varphi = (e^{-i\varphi \hat{Z}/2} \otimes \hat{1}_s) \hat{V}_0 (e^{i\varphi \hat{Z}/2} \otimes \hat{1}_s)$ and $\hat{Z} |\pm\rangle_b = |\mp\rangle_b$. Eq. (C5) essentially implements

$$\hat{V}_{\vec{\varphi}} = \bigoplus_{\lambda, \pm} \left(\hat{1}_b \mathcal{A}(\theta_\lambda) + i\hat{Z}_b \mathcal{B}(\theta_\lambda) + i\hat{X}_b \mathcal{C}(\theta_\lambda) + i\hat{Y}_b \mathcal{D}(\theta_\lambda) \right) \otimes |G_{\lambda\pm}\rangle\langle G_{\lambda\pm}|_{as}, \quad (\text{C6})$$

where $|G_{\lambda\pm}\rangle = (|G_\lambda\rangle \pm i|G_\lambda^\perp\rangle) / \sqrt{2}$ and $(\mathcal{A}, \mathcal{B}, \mathcal{C}, \mathcal{D})$ are real functions on θ_λ . We can classically solve for the vector $\vec{\varphi}$ to control each θ_λ thus implementing various functions of H . Before specifying the explicit constraints, we first state functions to be implemented in Hamiltonian simulation and USA.

1. Hamiltonian simulation (HS)

Given $\vec{\varphi} \in \mathbb{R}^K$, by choose $\Phi = \pi/2$ and projecting $\hat{V}_{\vec{\varphi}} |+\rangle_b |G\rangle_a$ on to $\langle G|_a \langle +|_b$, Eq. (C6) becomes

$$\langle G|_a \langle +|_b \hat{V}_{\vec{\varphi}} |+\rangle_b |G\rangle_a = \bigoplus_{\lambda} \left(\tilde{A}(\lambda) + i\tilde{C}(\lambda) \right) \otimes |\lambda\rangle\langle\lambda|_s, \quad (\text{C7})$$

where $\tilde{A}(\lambda) = \sum_{\text{even } k=0}^{K/2} a_k T_k(\lambda)$, $\tilde{C}(\lambda) = \sum_{\text{odd } k=1}^{K/2} c_k T_k(\lambda)$, and $a_k, c_k \in \mathbb{R}$ are coefficients depending on $\vec{\varphi}$.

Observe that U can be decomposed using the Jacobi-Anger expansion [38]

$$\begin{aligned} e^{-i\lambda t} &= J_0(t) + 2 \sum_{\text{even } k>0}^{\infty} (-1)^{\frac{k}{2}} J_k(t) T_k(\lambda) + i2 \sum_{\text{odd } k>0}^{\infty} (-1)^{\frac{k-1}{2}} J_k(t) T_k(\lambda) \\ &= A(\lambda) + iC(\lambda), \end{aligned} \quad (\text{C8})$$

where J_k is the Bessel function of the first kind and T_k are Chebyshev's polynomials. We truncate $A(\lambda)$ and $C(\lambda)$ in Eq. (C8) at order K , such that we need $\vec{\varphi} \in \mathbb{R}^{2K}$ to tune coefficients

$$\begin{aligned} \tilde{A}(\lambda) &= J_0(t) + 2 \sum_{\text{even } k>0}^K (-1)^{\frac{k}{2}} J_k(t) T_k(\lambda) \\ \tilde{C}(\lambda) &= 2 \sum_{\text{odd } k>0}^K (-1)^{\frac{k-1}{2}} J_k(t) T_k(\lambda). \end{aligned} \quad (\text{C9})$$

We will need the $\tilde{A}(\lambda)$ and $\tilde{C}(\lambda)$ to satisfy lemma 5, which gives how robust our function is when approximating $A(\lambda), C(\lambda)$ by $\tilde{A}(\lambda), \tilde{C}(\lambda)$.

Lemma 5. (lemma 14 of ref [2]) For any even integer $Q > 0$, a choice of functions $\mathcal{A}(\theta)$ and $\mathcal{C}(\theta)$ is achievable by the framework of QSP if and only if the following are true:

1. $\mathcal{A}(\theta) = \sum_{k=0}^K a_k \cos(k\theta)$ be a real cosine Fourier series of degree at most K , where a_k are coefficients;
2. $\mathcal{C}(\theta) = \sum_{k=1}^K c_k \sin(k\theta)$ be a real sine Fourier series of degree at most K , where c_k are coefficients;
3. $\mathcal{A}(0) = 1 + \epsilon_1$, where $|\epsilon_1| \leq 1$;
4. $\forall \theta \in \mathbb{R}, \mathcal{A}^2(\theta) + \mathcal{C}^2(\theta) \leq 1 + \epsilon_2$, where $\epsilon_2 \in [0, 1]$.

Then, with $\tilde{\epsilon} = \epsilon_1 + \epsilon_2$, we can approximate the evolution unitary e^{-iHt} with classically precomputed $\vec{\varphi} \in \mathbb{R}^{2K}$ such that

$$\left\| \langle +|_b \langle G|_a \hat{V}_{\vec{\varphi}} |G\rangle_a |+\rangle_b - e^{-iHt} \right\| \leq \mathcal{O}(\sqrt{\tilde{\epsilon}}). \quad (\text{C10})$$

The post-selection succeeds with probability at least $1 - 2\sqrt{\tilde{\epsilon}}$.

Note $\mathcal{A}(\theta)$ maximized at $\theta = 0$. ϵ_1 quantifies the truncation error because $\max_{\lambda} \tilde{A}(\lambda) = 1$ only if $K \rightarrow \infty$. Furthermore, ϵ_2 quantifies the rescaling error for the mixed-in term, i.e. V_2 . As we amplify part of it by $1/(1-p)$, the magnitude of $\hat{V}_{\vec{\varphi}}$ may exceed 1 in such instance.

To implement RTS, we first decide the type of QSP according to classical computation power. A type 2 QSP realizes the Hamiltonian evolution in a single unitary. Therefore, we need to truncate Eq. (C9) at a very high K as the precision scales linear with evolution time. Consequently, the calculation of $\vec{\varphi}$ becomes extremely hard. On the other hand, a type 1 QSP splits the evolution time into segments and concatenates these short-time evolutions to approximate the overall Hamiltonian dynamic. Whereas it faces the problem of large constant overhead. RTS embraces both cases as discussed in the main text. In the following discussion, we will give constructions of the two unitaries we are mixing. We drop the subscript $\vec{\varphi}$ in $\hat{V}_{\vec{\varphi}}$ for simplicity, and denote \hat{V}_1 and \hat{V}_2 as the two unitaries, where

$$\begin{aligned}
\hat{V}_1(\lambda) &= A_1(\lambda) + iC_1(\lambda) \\
&= J_0(t) + 2 \sum_{\text{even } k>0}^{K_1} (-1)^{\frac{k}{2}} J_k(t) T_k(\lambda) + i2 \sum_{\text{odd } k>0}^{K_1} (-1)^{\frac{k-1}{2}} J_k(t) T_k(\lambda) \\
\hat{V}_2(\lambda) &= A_2(\lambda) + iC_2(\lambda) \\
&= J_0(t) + 2 \sum_{\text{even } k>0}^{K_1} (-1)^{\frac{k}{2}} J_k(t) T_k(\lambda) + \frac{1}{1-p} \left(2 \sum_{\text{even } k>K_1}^{K_2} (-1)^{\frac{k}{2}} J_k(t) T_k(\lambda) \right) \\
&\quad + i2 \sum_{\text{odd } k>0}^{K_1} (-1)^{\frac{k-1}{2}} J_k(t) T_k(\lambda) + i \frac{1}{1-p} \left(2 \sum_{\text{odd } k>K_1}^{K_2} (-1)^{\frac{k-1}{2}} J_k(t) T_k(\lambda) \right) \\
\hat{V}_m(\lambda) &= p\hat{V}_1(\lambda) + (1-p)\hat{V}_2(\lambda) \\
&= (pA_1(\lambda) + (1-p)A_2(\lambda)) + i(pC_1(\lambda) + (1-p)C_2(\lambda)) \\
&= A_m(\lambda) + iC_m(\lambda).
\end{aligned} \tag{C11}$$

To approximate $\{A_i, C_i | i \in \{1, 2, m\}\}$ by the rescaled function $\{\tilde{A}_i, \tilde{C}_i | i \in \{1, 2, m\}\}$ with lemma 5, we need to explicitly calculate the corresponding ϵ_1 and ϵ_2 .

Lemma 6. (Truncation and rescaling error)

For index $i = \{1, 2, m\}$, we can upper bound

$$\max_{\lambda} |(A_i + iC_i) - (\tilde{A}_i + i\tilde{C}_i)| \tag{C12}$$

by $\mathcal{O}(\sqrt{|\epsilon_{1,V_i}| + \epsilon_{2,V_i}})$ where $\epsilon_{1,V_i} := \tilde{A}_i(0) - 1$ and $\epsilon_{2,V_i} := \max_{\lambda} \tilde{A}^2(\lambda) + \tilde{C}^2(\lambda) - 1$.

1.

$$\epsilon_{1,V_1} \leq \frac{4t^{K_1}}{2^{K_1} K_1!}, \quad \epsilon_{2,V_1} = 0 \tag{C13}$$

2.

$$\epsilon_{1,V_2} \leq \frac{p}{1-p} \frac{4t^{K_1}}{2^{K_1} K_1!}, \quad \epsilon_{2,V_2} = 2\epsilon_{1,V_1} + \left(\frac{J_0(t)}{2} + \frac{4}{p(1-p)} \right) \epsilon_{1,V_2} \tag{C14}$$

3. For the mixed function, $V_m = pV_1 + (1-p)V_2$, we have

$$\epsilon_{1,V_m} \leq \frac{4t^{K_2}}{2^{K_2} K_2!}, \quad \epsilon_{2,V_m} = 0 \tag{C15}$$

Proof. 1. proof for \hat{V}_1

ϵ_{1,V_1} is the truncation error in equation ((C9)) with $K = K_1$. Since λ originated from a cosine function in the Chebyshev polynomial, it takes the value $\lambda \in [-1, 1]$, and we maximize the truncation error over the domain to obtain an upper bound on ϵ_{1,V_1} . Thus,

$$\begin{aligned}
\epsilon_{1,V_1} &\leq \max_{\lambda \in [-1, 1]} \left| e^{-i\lambda t} - (\tilde{A}_1(\lambda) + i\tilde{C}_1(\lambda)) \right| \\
&= \max_{\lambda \in [-1, 1]} \left| 2 \sum_{\text{even } k=1}^{K_1} (-1)^{\frac{k}{2}} J_k(t) T_k(\lambda) + i2 \sum_{\text{odd } k=1}^{K_1} (-1)^{\frac{k-1}{2}} J_k(t) T_k(\lambda) \right| \\
&\leq 2 \sum_{k=1}^{K_1} |J_k(t)| \leq \frac{4t^{K_1}}{2^{K_1} K_1!}.
\end{aligned} \tag{C16}$$

It is trivial that $\tilde{A}_1^2(\lambda) + \tilde{C}_1^2(\lambda) \leq A^2(\lambda) + C^2(\lambda) = 1, \forall K_1 \in \mathbb{Z}$. Thus $\epsilon_{2,V_1} = 0$

2. Proof for \hat{V}_2

Similarly, we obtain

$$\begin{aligned}
\epsilon_{1,V_2} &\leq \max_{\lambda \in [-1,1]} \left| e^{-i\lambda t} - \left(\tilde{A}_2(\lambda) + i\tilde{C}_2(\lambda) \right) \right| \\
&= \max_{\lambda \in [-1,1]} \left| -\frac{p}{1-p} \left(2 \sum_{\text{even } k > K_1}^{K_2} (-1)^{\frac{k}{2}} J_k(t) T_k(\lambda) + i2 \sum_{\text{odd } k > K_1}^{K_2} (-1)^{\frac{k-1}{2}} J_k(t) T_k(\lambda) \right) \right. \\
&\quad \left. + 2 \sum_{\text{even } k > K_2}^{\infty} (-1)^{\frac{k}{2}} J_k(t) T_k(\lambda) + i2 \sum_{\text{odd } k > K_2}^{\infty} (-1)^{\frac{k-1}{2}} J_k(t) T_k(\lambda) \right| \\
&\leq \frac{p}{1-p} \left(2 \sum_{k > K_1}^{K_2} |J_k(t)| \right) - 2 \sum_{k > K_2}^{\infty} |J_k(t)| \\
&= \frac{p}{1-p} \left(2 \sum_{k > K_1}^{\infty} |J_k(t)| \right) - \left(2 + \frac{p}{1-p} \right) \sum_{k > K_2}^{\infty} |J_k(t)| \\
&\leq \frac{p}{1-p} \frac{4t^{K_1}}{2^{K_1} K_1!}.
\end{aligned} \tag{C17}$$

It should be noticed that ϵ_{2,V_2} will be greater than zero as we increase p for a given K_2 . We have to find ϵ_{2,V_2} satisfying

$$\begin{aligned}
\epsilon_{2,V_2} &\leq \left| 1 - \left(\tilde{A}_2^2(\lambda) + \tilde{C}_2^2(\lambda) \right) \right| \\
&= \left| (A^2(\lambda) - \tilde{A}_2^2(\lambda)) + (C^2(\lambda) - \tilde{C}_2^2(\lambda)) \right|.
\end{aligned} \tag{C18}$$

For simplicity, we abbreviate the sum by $2 \sum_{\text{even } k > m}^n (-1)^{\frac{k}{2}} J_k(t) T_k(\lambda) = \mathfrak{S}_m^n(\lambda)$ and compute the first parentheses in equation ((C18)) as

$$\begin{aligned}
&A^2(\lambda) - \tilde{A}_2^2(\lambda) \\
&= (J_0(t) + \mathfrak{S}_0^\infty(\lambda))^2 - \left(J_0(t) + \mathfrak{S}_0^{K_1}(\lambda) + \frac{1}{1-p} (\mathfrak{S}_{K_1}^{K_2}(\lambda)) \right)^2 \\
&= 2J_0(t)\mathfrak{S}_0^\infty(\lambda) + (\mathfrak{S}_0^\infty(\lambda))^2 - 2J_0(t) \left(\mathfrak{S}_0^{K_1}(\lambda) + \frac{1}{1-p} (\mathfrak{S}_{K_1}^{K_2}(\lambda)) \right) - \left(\mathfrak{S}_0^{K_1}(\lambda) + \frac{1}{1-p} (\mathfrak{S}_{K_1}^{K_2}(\lambda)) \right)^2 \\
&= 2J_0 \left(\mathfrak{S}_0^\infty(\lambda) - \mathfrak{S}_0^{K_1}(\lambda) - \frac{1}{1-p} (\mathfrak{S}_{K_1}^{K_2}(\lambda)) \right) + (\mathfrak{S}_0^\infty(\lambda))^2 - \left(\mathfrak{S}_0^{K_1}(\lambda) + \frac{1}{1-p} (\mathfrak{S}_{K_1}^{K_2}(\lambda)) \right)^2 \\
&= 2J_0 \delta_s + \left(\mathfrak{S}_0^\infty(\lambda) + \mathfrak{S}_0^{K_1}(\lambda) + \frac{1}{1-p} (\mathfrak{S}_{K_1}^{K_2}(\lambda)) \right) \left(\mathfrak{S}_0^\infty(\lambda) - \mathfrak{S}_0^{K_1}(\lambda) - \frac{1}{1-p} (\mathfrak{S}_{K_1}^{K_2}(\lambda)) \right) \\
&\leq (2J_0 + 3)\delta_s,
\end{aligned} \tag{C19}$$

where

$$\begin{aligned}
|\delta_s| &= \left| \mathfrak{S}_0^\infty(\lambda) - \mathfrak{S}_0^{K_1}(\lambda) - \frac{1}{1-p} (\mathfrak{S}_{K_1}^{K_2}(\lambda)) \right| \\
&= \left| -\frac{p}{1-p} \mathfrak{S}_0^\infty(\lambda) + \frac{1}{1-p} \mathfrak{S}_{|2\rangle}^\infty(\lambda) \right| \\
&\leq \frac{p}{1-p} \mathfrak{S}_0^\infty(\lambda).
\end{aligned} \tag{C20}$$

Similarly, with definition $2 \sum_{\text{odd } k > m}^n (-1)^{\frac{k-1}{2}} J_k(t) T_k(\lambda) = \mathfrak{K}_m^n(\lambda)$ we have

$$\begin{aligned}
&C^2(\lambda) - \tilde{C}_2^2(\lambda) \\
&\approx 3\delta_k,
\end{aligned} \tag{C21}$$

where

$$\begin{aligned} |\delta_k| &= \left| \mathfrak{K}_0^\infty(\lambda) - \mathfrak{K}_0^{K_1}(\lambda) - \frac{1}{1-p} \left(\mathfrak{K}_{K_1}^{K_2}(\lambda) \right) \right| \\ &\leq \frac{p}{1-p} \mathfrak{K}_{K_1}^\infty(\lambda). \end{aligned} \quad (\text{C22})$$

Observe that

$$\delta_s + \delta_k \leq \frac{p}{1-p} \frac{4t^{K_1}}{2^{K_1} K_1!} \quad (\text{C23})$$

and $J_0(t) \leq 1, \forall t$, we finally bound

$$\epsilon_{2,V_2} \leq (2J_0 + 3)\delta_s + 3\delta_k \leq \frac{5p}{1-p} \frac{4t^{K_1}}{2^{K_1} K_1!}. \quad (\text{C24})$$

3. Proof for \hat{V}_m Observe that $V_m = pV_1 + (1-p)V_2 = J_0(t) + 2 \sum_{\text{even } k > 0}^{K_2} (-1)^{k/2} J_k(t) T_k(\lambda) + i2 \sum_{\text{odd } k > 0}^{K_2} (-1)^{(k-1)/2} J_k(t) T_k(\lambda)$, we have

$$\epsilon_{1,V_m} \leq \frac{4t^{K_2}}{2^{K_2} K_2!} \text{ and } \epsilon_{2,V_m} = 0 \quad (\text{C25})$$

□

We can now proof the error bound on Hamiltonian simulation with QSP with lemma 6 and 5

Theorem 5. Consider two quantum circuits implementing \hat{V}_1 and \hat{V}_2 in Eq. (C11). Given a mixing probability $p \in [0, 1)$ and an arbitrary density matrix ρ , distance between the evolved state under the mixing channel $\mathcal{V}_{\text{mix}}(\rho) = pV_1\rho V_1^\dagger + (1-p)V_2\rho V_2^\dagger$ and an ideal evolution for U_λ is bounded by

$$\|\mathcal{V}_{\text{mix}}(\rho) - U\rho U^\dagger\| \leq \max \left\{ 28\delta_1, 8\sqrt{\delta_m} \right\}, \quad (\text{C26})$$

where $\delta_m = \frac{4t^{K_2}}{2^{K_2} K_2!}$ and $\delta_1 = \frac{4t^{K_1}}{2^{K_1} K_1!}$. The overall cost of implementing this segment is

$$G = \mathcal{O}(dt\|H\|_{\text{max}} + (pK_1 + (1-p)K_2)), \quad (\text{C27})$$

where d is the sparsity of H , and K_1 and K_2 are truncated order in V_1 and V_2 respectively. The failure probability is upper bounded by $\xi \geq 4p\sqrt{\delta_2}$.

Proof. The error of mixing channel in lemma 1.

$$\begin{aligned} \epsilon &= 4b + 2pa_1^2 + 2(1-p)a_2^2 \\ &= 4\sqrt{\frac{4t^{K_2}}{2^{K_2} K_2!}} + 2p\frac{4t^{K_1}}{2^{K_1} K_1!} + 2(1-p)\frac{6p}{1-p} \frac{4t^{K_1}}{2^{K_1} K_1!} \\ &\leq 4\sqrt{\frac{4t^{K_2}}{2^{K_2} K_2!}} + 14\frac{4t^{K_1}}{2^{K_1} K_1!} \\ &\leq \max \left\{ 8\sqrt{\frac{4t^{K_2}}{2^{K_2} K_2!}}, 28\frac{4t^{K_1}}{2^{K_1} K_1!} \right\}. \end{aligned} \quad (\text{C28})$$

We can lower bound the failure probability ξ using the lemma 1 and 5 such that

$$\begin{aligned} \xi &\leq 2pa_1 + 2(1-p)a_2 \\ &= 2p\sqrt{\frac{4t^{K_1}}{2^{K_1} K_1!}} + 2\sqrt{6p(1-p)}\sqrt{\frac{4t^{K_1}}{2^{K_1} K_1!}} \\ &\leq 4p\sqrt{\frac{4t^{K_1}}{2^{K_1} K_1!}}. \end{aligned} \quad (\text{C29})$$

□

2. Uniform spectral amplification (USA)

Going back to Eq. (C6), with another ancilla qubit in \mathcal{H}_c , we can define

$$\hat{W}_{\vec{\varphi}} = \hat{V}_{\vec{\varphi}} \otimes |+\rangle\langle+|_c + \hat{V}_{\pi-\vec{\varphi}} \otimes |-\rangle\langle-|_c. \quad (\text{C30})$$

We then can project $\hat{W}_{\vec{\varphi}} |G\rangle_a |0\rangle_b |0\rangle_c$ onto $\langle 0|_c |0\rangle_b |G\rangle_a$ such that

$$\langle 0|_c \langle 0|_b \langle G|_a \hat{W}_{\vec{\varphi}} |G\rangle_a |0\rangle_b |0\rangle_c = D(\lambda) \otimes |\lambda\rangle\langle\lambda|, \quad (\text{C31})$$

where D is an odd real polynomial function of degree at most $2K+1$ satisfying $\forall \lambda \in [-1, 1], D^2(\lambda) \leq 1$. The rescaling in this case becomes easy because we can neglect A, B and C in Eq. (C6). For the mix-in term, where the norm may be greater than 1, we can simply rescale it by a constant factor, and the upper bound on the corresponding error will be doubled.

In the task of USA, we would like to approximate the truncated linear function

$$f_{\Gamma, \delta}(\lambda) = \begin{cases} \frac{\lambda}{2\Gamma}, & |\lambda| \in [0, \Gamma] \\ \in [-1, 1], & |\lambda| \in (\Gamma, 1], \end{cases} \quad (\text{C32})$$

where $\delta = \max_{|x| \in [0, \Gamma]} \left| \frac{|x|}{2\Gamma} \tilde{f}_{\Gamma}(\lambda) - 1 \right|$ is the maximum error tolerance.

We can approximate Eq. (C32) by

$$f_{\Gamma, \delta}(\lambda) = \frac{\lambda}{4\Gamma} \left(\text{erf} \left(\frac{\lambda + 2\Gamma}{\sqrt{2}\Gamma\delta'} \right) + \text{erf} \left(\frac{2\Gamma - \lambda}{\sqrt{2}\Gamma\delta'} \right) \right), \quad (\text{C33})$$

where $1/\delta' = \sqrt{\log(2/(\pi\delta^2))}$ and $\text{erf}(\gamma x) = \frac{2}{\pi} \int_0^{\gamma x} e^{-t^2} dt = \frac{2}{\sqrt{\pi}} \int_0^x e^{-(\gamma t)^2} dt$ is the error function. Observe that we can approximate the truncated linear function by a combination of error functions only. The following is the construction of the error function by Chebyshev's polynomial using the truncated Jacobi-Anger expansion

$$P_{\text{erf}, \gamma, K_1}(\lambda) = \frac{2\gamma e^{-\gamma^2/2}}{\sqrt{\pi}} \left(J_0 \left(\frac{\gamma^2}{2} \right) \lambda + \sum_{k=1}^{(K_1-1)/2} J_k \left(\frac{\gamma^2}{2} \right) (-1)^k \left(\frac{T_{2k+1}(\lambda)}{2k+1} - \frac{T_{2k-1}(\lambda)}{2k-1} \right) \right). \quad (\text{C34})$$

The polynomial we mixed in with small probability is

$$\begin{aligned} P_{\text{erf}, \gamma, K_2}(\lambda) = & \frac{2\gamma e^{-\gamma^2/2}}{\sqrt{\pi}} \left(J_0 \left(\frac{\gamma^2}{2} \right) \lambda + \left(\sum_{k=1}^{(K_1-1)/2} J_k \left(\frac{\gamma^2}{2} \right) (-1)^k \left(\frac{T_{2k+1}(\lambda)}{2k+1} - \frac{T_{2k-1}(\lambda)}{2k-1} \right) \right) \right. \\ & \left. + \frac{1}{1-p} \left(\sum_{k=(K_1+1)/2}^{(K_2-1)/2} J_k \left(\frac{\gamma^2}{2} \right) (-1)^k \left(\frac{T_{2k+1}(\lambda)}{2k+1} - \frac{T_{2k-1}(\lambda)}{2k-1} \right) \right) \right), \end{aligned} \quad (\text{C35})$$

We can then substitute Eq. (C34) and (C35) into Eq. (C33) to approximate truncated linear function, which results in $\hat{P}_{\Gamma, \delta, K_{1(2)}}$ for replacing $\text{erf}(\lambda)$ by $P_{\text{erf}, \gamma, K_{1(2)}}(\lambda)$

$$\hat{P}_{\Gamma, \delta, K_{1(2)}}(\lambda) = \frac{\lambda}{4\Gamma} \left(P_{\text{erf}, \gamma, K_{1(2)}} \left(\frac{\lambda + 2\Gamma}{\sqrt{2}\Gamma\delta'} \right) + P_{\text{erf}, \gamma, K_{1(2)}} \left(\frac{2\Gamma - \lambda}{\sqrt{2}\Gamma\delta'} \right) \right). \quad (\text{C36})$$

Follow the error propagation in ref. [3], we can bound

$$\epsilon_{\Gamma, K} = \max_{|\lambda| \in [0, \Gamma]} \frac{2\Gamma}{|\lambda|} \left| \hat{P}_{\Gamma, \delta, K}(\lambda) - \frac{\lambda}{2\Gamma} \right| \leq 2\epsilon_{\text{erf}, 4\Gamma, K-1}, \quad (\text{C37})$$

where $\epsilon_{\text{erf}, \Gamma, K}$ is the truncation error of $P_{\text{erf}, \gamma, K}(\lambda)$ approximating $\text{erf}(\gamma\lambda)$.

Lemma 7. (Truncation error of approximating error function)

Polynomial functions, $P_{\text{erf},\gamma,K_1}(\lambda)$ and $P_{\text{erf},\gamma,K_2}(\lambda)$, constructed by Jacobi-Anger expansion and their probability mixture, $P_{\text{erf},\gamma,p,K_1,K_2}(\lambda) = pP_{\text{erf},\gamma,K_1}(\lambda) + (1-p)P_{\text{erf},\gamma,K_2}(\lambda)$, $p \in [0, 1]$ approximate the error function $\text{erf}(\gamma\lambda) = \frac{2}{\pi} \int_0^{\gamma\lambda} e^{-t^2} dt$ with truncation error bounded by a'_1 , a'_2 and b respectively.

$$\begin{aligned} a'_1 &= \frac{\gamma e^{-\gamma^2/2}}{\sqrt{\pi}} \frac{4(\gamma^2/2)^{(K_1+1)/2}}{2^{(K_1+1)/2}((K_1+1)/2)!} \\ a'_2 &= \frac{p}{1-p} \frac{\gamma e^{-\gamma^2/2}}{\sqrt{\pi}} \frac{4(\gamma^2/2)^{(K_1+1)/2}}{2^{(K_1+1)/2}((K_1+1)/2)!} \\ b' &= \frac{\gamma e^{-\gamma^2/2}}{\sqrt{\pi}} \frac{4(\gamma^2/2)^{(K_2+1)/2}}{2^{(K_2+1)/2}((K_2+1)/2)!} \end{aligned} \quad (\text{C38})$$

Proof. Calculate that

$$1. |\text{erf}(\lambda) - P_{\text{erf},\gamma,K_1}(\lambda)| \leq a'_1$$

$$\begin{aligned} \epsilon_{\text{erf},\gamma,K_1} &= |\text{erf}(\lambda) - P_{\text{erf},\gamma,K_1}(\lambda)| \\ &= \left| \frac{2\gamma e^{-\gamma^2/2}}{\sqrt{\pi}} \sum_{k=(K_1+1)/2}^{\infty} J_k\left(\frac{\gamma^2}{2}\right) (-1)^k \left(\frac{T_{2k+1}(\lambda)}{2k+1} - \frac{T_{2k-1}(\lambda)}{2k-1} \right) \right| \\ &\leq \frac{2\gamma e^{-\gamma^2/2}}{\sqrt{\pi}} \sum_{k=(K_1+1)/2}^{\infty} \left| J_k\left(\frac{\gamma^2}{2}\right) \right| \left(\frac{1}{2k+1} - \frac{1}{2k-1} \right) \\ &\leq \frac{2\gamma e^{-\gamma^2/2}}{\sqrt{\pi}} \sum_{k=(K_1+1)/2}^{\infty} \left| J_k\left(\frac{\gamma^2}{2}\right) \right| \\ &\leq \frac{\gamma e^{-\gamma^2/2}}{\sqrt{\pi}} \frac{4(\gamma^2/2)^{(K_1+1)/2}}{2^{(K_1+1)/2}((K_1+1)/2)!} =: a'_1 \end{aligned} \quad (\text{C39})$$

$$2. |\text{erf}(\lambda) - P_{\text{erf},\gamma,K_2}(\lambda)| \leq a'_2$$

$$\begin{aligned} \epsilon_{\text{erf},\gamma,K_2} &= |\text{erf}(\lambda) - P_{\text{erf},\gamma,K_2}(\lambda)| \\ &= \left| \frac{2\gamma e^{-\gamma^2/2}}{\sqrt{\pi}} \left(-\frac{p}{1-p} \sum_{k=(K_1+1)/2}^{(K_2-1)/2} J_k\left(\frac{\gamma^2}{2}\right) (-1)^k \left(\frac{T_{2k+1}(\lambda)}{2k+1} - \frac{T_{2k-1}(\lambda)}{2k-1} \right) \right. \right. \\ &\quad \left. \left. + \sum_{k=(K_2+1)/2}^{\infty} J_k\left(\frac{\gamma^2}{2}\right) (-1)^k \left(\frac{T_{2k+1}(\lambda)}{2k+1} - \frac{T_{2k-1}(\lambda)}{2k-1} \right) \right) \right| \\ &\leq \left| \frac{2\gamma e^{-\gamma^2/2}}{\sqrt{\pi}} \left(-\frac{p}{1-p} \sum_{k=(K_1+1)/2}^{\infty} J_k\left(\frac{\gamma^2}{2}\right) (-1)^k \left(\frac{T_{2k+1}(\lambda)}{2k+1} - \frac{T_{2k-1}(\lambda)}{2k-1} \right) \right. \right. \\ &\quad \left. \left. + \left(1 + \frac{p}{1-p}\right) \sum_{k=(K_2+1)/2}^{\infty} J_k\left(\frac{\gamma^2}{2}\right) (-1)^k \left(\frac{T_{2k+1}(\lambda)}{2k+1} - \frac{T_{2k-1}(\lambda)}{2k-1} \right) \right) \right| \\ &\leq \frac{p}{1-p} \frac{2\gamma e^{-\gamma^2/2}}{\sqrt{\pi}} \sum_{k=(K_1+1)/2}^{\infty} \left| J_k\left(\frac{\gamma^2}{2}\right) \right| \\ &\leq \frac{p}{1-p} \frac{\gamma e^{-\gamma^2/2}}{\sqrt{\pi}} \frac{4(\gamma^2/2)^{(K_1+1)/2}}{2^{(K_1+1)/2}((K_1+1)/2)!} =: a'_2 \end{aligned} \quad (\text{C40})$$

$$3. |erf(\lambda) - P_{erf,\gamma,p,K_1,K_2}(\lambda)| \leq b'$$

$$\begin{aligned}
\epsilon_{erf,\gamma,p,K_1,K_2}(\lambda) &= |erf(\lambda) - P_{erf,\gamma,p,K_1,K_2}(\lambda)| \\
&= \left| \frac{2\gamma e^{-\gamma^2/2}}{\sqrt{\pi}} \sum_{k=(K_2+1)/2}^{\infty} J_k\left(\frac{\gamma^2}{2}\right) (-1)^k \left(\frac{T_{2k+1}(\lambda)}{2k+1} - \frac{T_{2k-1}(\lambda)}{2k-1} \right) \right| \\
&\leq \frac{2\gamma e^{-\gamma^2/2}}{\sqrt{\pi}} \sum_{k=(K_2+1)/2}^{\infty} \left| J_k\left(\frac{\gamma^2}{2}\right) \right| \left(\frac{1}{2k+1} - \frac{1}{2k-1} \right) \\
&\leq \frac{2\gamma e^{-\gamma^2/2}}{\sqrt{\pi}} \sum_{k=(K_2+1)/2}^{\infty} \left| J_k\left(\frac{\gamma^2}{2}\right) \right| \\
&\leq \frac{\gamma e^{-\gamma^2/2}}{\sqrt{\pi}} \frac{4(\gamma^2/2)^{(K_2+1)/2}}{2^{(K_2+1)/2}((K_2+1)/2)!} =: b'
\end{aligned} \tag{C41}$$

□

We can then upper bound the error of approximating the truncated linear function

Lemma 8. (Truncation error of approximating linear function)

Polynomial functions $\hat{P}_{\Gamma,\delta,K_{1(2)}}(\lambda)$ in Eq. (C36) and the probability mixture $\hat{P}_{\Gamma,\delta,p,K_1,K_2}(\lambda) = p\hat{P}_{\Gamma,\delta,K_1}(\lambda) + (1-p)\hat{P}_{\Gamma,\delta,K_2}(\lambda)$, $p \in [0, 1]$ approximate the truncated linear function $f_{\Gamma,\delta}(\lambda) = \lambda/(2\Gamma)$, $|\lambda| \in [0, \Gamma]$ with truncation error bounded by a_1 , a_2 and b respectively.

$$\begin{aligned}
a_1 &= \frac{8\Gamma e^{-8\Gamma^2}}{\sqrt{\pi}} \frac{4(8\Gamma^2)^{K_1/2}}{2^{K_1/2}(K_1/2)!} \\
a_2 &= \frac{p}{1-p} \frac{8\Gamma e^{-8\Gamma^2}}{\sqrt{\pi}} \frac{4(8\Gamma^2)^{K_1/2}}{2^{K_1/2}(K_1/2)!} = \frac{p}{1-p} a_1 \\
b &= \frac{8\Gamma e^{-8\Gamma^2}}{\sqrt{\pi}} \frac{4(8\Gamma^2)^{K_2/2}}{2^{K_2/2}(K_2/2)!}
\end{aligned} \tag{C42}$$

Proof. This is followed by substituting Eq. (C37) into lemma 7. □

Theorem 6. (QSP implementation of USA)

For the unitary $\hat{W}_{\vec{\varphi}_{1(2)}}$ and post-selection scheme in Eq. (C31), there exist two sets of angles $\vec{\varphi}_{1(2)}$ such that $D_{1(2)}(\lambda) = \hat{P}_{\Gamma,\delta,K_{1(2)}}(\lambda)$. Denote these two quantum circuits as V_1 and V_2 respectively. Then, given a mixing probability $p \in [0, 1]$ and an arbitrary density matrix ρ , distance between the evolved state under the mixing channel $\mathcal{V}_{mix}(\rho) = pV_1\rho V_1^\dagger + (1-p)V_2\rho V_2^\dagger$ and an ideal transformation implementing the transformation given by Eq. (C32) is bounded by

$$\|\mathcal{V}_{mix}(\rho) - f_{\Gamma,\delta}(\rho)\| \leq \max \left\{ 8b, \frac{4}{1-p} a_1^2 \right\}, \tag{C43}$$

where $a_1 = \frac{8\Gamma e^{-8\Gamma^2}}{\sqrt{\pi}} \frac{4(8\Gamma^2)^{K_1/2}}{2^{K_1/2}(K_1/2)!}$ and $b = \frac{8\Gamma e^{-8\Gamma^2}}{\sqrt{\pi}} \frac{4(8\Gamma^2)^{K_2/2}}{2^{K_2/2}(K_2/2)!}$. The overall cost of implementing this segment is

$$G = \mathcal{O}(dt\|H\|_{max} + (pK_1 + (1-p)K_2)), \tag{C44}$$

where d is the sparsity of H , and K_1 and K_2 are truncated order in V_1 and V_2 respectively.

Proof. With two classically computed $\vec{\varphi}_1 \in \mathbb{R}^{2K_1+1}$, $\vec{\varphi}_2 \in \mathbb{R}^{2K_2+1}$, we can implement $\hat{W}_{\vec{\varphi}_{1(2)}}$ and $\hat{W}_{\vec{\varphi}_m} = p\hat{W}_{\vec{\varphi}_1} + (1-p)\hat{W}_{\vec{\varphi}_2}$ such that they approximate an unitary U implementing truncated linear amplification by bounded errors

$$\begin{aligned}
\| \langle 0|_c \langle 0|_b \langle G|_a \hat{W}_{\vec{\varphi}_1} |G\rangle_a |0\rangle_b |0\rangle_c - U \| &\leq a_1 \\
\| \langle 0|_c \langle 0|_b \langle G|_a \hat{W}_{\vec{\varphi}_2} |G\rangle_a |0\rangle_b |0\rangle_c - U \| &\leq a_2 \\
\| \langle 0|_c \langle 0|_b \langle G|_a \hat{W}_{\vec{\varphi}_m} |G\rangle_a |0\rangle_b |0\rangle_c - U \| &\leq b
\end{aligned} \tag{C45}$$

The operator norm further bound the state distance after quantum channels since $\|V\rho V^\dagger - U\rho U^\dagger\| \leq \|V - U\|, \forall \rho$. Employing lemma 1 gives the final result since b is exponentially smaller than $a_{1(2)}$, i.e.

$$\begin{aligned} \|\mathcal{V}_{mix}(\rho) - U\rho U^\dagger\| &\leq 4b + 2pa_1^2 + 2(1-p)a_2^2 \\ &\leq \max \left\{ 8b, \frac{4}{1-p}a_1^2 \right\} \end{aligned} \quad (\text{C46})$$

□

Appendix D: Application in ODE

Consider a differential equation of the form

$$\frac{d\vec{x}}{dt} = A\vec{x} + \vec{b}, \quad (\text{D1})$$

where $A \in \mathbb{R}^{n \times n}$, $\vec{b} \in \mathbb{R}^n$ are time-independent. The exact solution is given by

$$\vec{x}(t) = e^{At}\vec{x}(0) + (e^{At} - \mathbb{1}_n)A^{-1}\vec{b}, \quad (\text{D2})$$

where $\mathbb{1}_n$ is the n -dimensional identity vector.

We can approximate e^z and $(e^z - \mathbb{1}_n)z^{-1}$ by two k -truncated Taylor expansions:

$$T_k(z) := \sum_{k=0}^K \frac{z^k}{k!} \approx e^z \quad (\text{D3})$$

and

$$S_k(z) := \sum_{k=1}^K \frac{z^{k-1}}{k!} \approx (e^z - 1)z^{-1}. \quad (\text{D4})$$

Consider a short time h , We can approximate the solution $\vec{x}(qh)$ recursively from $\vec{x}((q-1)h)$, for an integer q . Denote x^q as the solution approximated by the algorithm, we have

$$x^{q+1} = T_k(Ah)x^q + S_k(Ah)h\vec{b}. \quad (\text{D5})$$

Furthermore, we can embed the series of recursive equations into a large linear system \mathcal{L} as proposed in [8] such that the solution to \mathcal{L} gives the history state [41] of x , which encodes solution at all time steps. \mathcal{L} has the form

$$C_{m,K,p}(Ah)|x\rangle = |0\rangle|x_{in}\rangle + h \sum_{i=0}^{m-1} |i(K+1)+1\rangle|b\rangle, \quad (\text{D6})$$

where m is the maximum time step and p is the repetition number of identity operator after evolution aiming to increase the probability of projecting onto the final state. The operator has the form

$$\begin{aligned} C_{m,K_1,p}(A) &:= \sum_{j=0}^{d_1} |j\rangle\langle j| \otimes \mathbb{1} - \sum_{i=0}^{m-1} \sum_{j=1}^{K_1} |i(K_1+1)+j\rangle\langle i(K_1+1)+j-1| \otimes \frac{A}{j} \\ &\quad - \sum_{i=0}^{m-1} \sum_{j=0}^{K_1} |(i+1)(K_1+1)\rangle\langle i(K_1+1)+j| \otimes \mathbb{1} - \sum_{j=d-p+1}^d |j\rangle\langle j-1| \otimes \mathbb{1}, \end{aligned} \quad (\text{D7})$$

where $d_1 = m(K_1+1) + p$. To implement RTS, we need to apply the modified higher order terms in Eq. (D3) and (D4). This could be done by performing the operator

$$\begin{aligned} \tilde{C}_{m,K_1,K_2,p}(A) &:= \sum_{j=0}^{d_2} |j\rangle\langle j| \otimes \mathbb{1} - \sum_{i=0}^{m-1} \sum_{j=1}^{K_1} |i(K_1+1)+j\rangle\langle i(K_1+1)+j-1| \otimes \frac{A}{j} \\ &\quad - \frac{1}{(1-p)^{1/(K_2-K_1-1)}} \sum_{i=0}^{m-1} \sum_{j=K_1+1}^{K_2} |i(K_2+1)+j\rangle\langle i(K_2+1)+j-1| \otimes \frac{A}{j} \\ &\quad - \sum_{i=0}^{m-1} \sum_{j=0}^{K_2} |(i+1)(K_2+1)\rangle\langle i(K_2+1)+j| \otimes \mathbb{1} - \sum_{j=d-p+1}^d |j\rangle\langle j-1| \otimes \mathbb{1}. \end{aligned} \quad (\text{D8})$$

\mathcal{L} with $C_{m,k,p}(Ah)$ and $\tilde{C}_{m,K_1,K_2,p}(Ah)$ gives solutions $|x\rangle$ and $|\tilde{x}\rangle$ respectively, where

- $|x_{i,j}\rangle$ satisfies

$$\begin{aligned}
 |x_{0,0}\rangle &= |x_{in}\rangle, \\
 |x_{i,0}\rangle &= \sum_{j=0}^{K_1} |x_{i-1,j}\rangle, \quad 1 \leq i \leq m \\
 |x_{i,1}\rangle &= Ah |x_{i,0}\rangle + h |b\rangle, \quad 0 \leq i < m \\
 |x_{i,j}\rangle &= \frac{Ah}{j} |x_{i,j-1}\rangle, \quad 0 \leq i < m, 2 \leq j \leq K_1 \\
 |x_{m,j}\rangle &= |x_{m,j_1}\rangle, \quad 1 \leq j \leq p
 \end{aligned} \tag{D9}$$

- $|\tilde{x}_{i,j}\rangle$ satisfies

$$\begin{aligned}
 |\tilde{x}_{0,0}\rangle &= |\tilde{x}_{in}\rangle, \\
 |\tilde{x}_{i,0}\rangle &= \sum_{j=0}^{K_2} |\tilde{x}_{i-1,j}\rangle, \quad 1 \leq i \leq m \\
 |\tilde{x}_{i,1}\rangle &= Ah |\tilde{x}_{i,0}\rangle + h |b\rangle, \quad 0 \leq i < m \\
 |\tilde{x}_{i,j}\rangle &= \frac{Ah}{j} |\tilde{x}_{i,j-1}\rangle, \quad 0 \leq i < m, 2 \leq j \leq K_1 \\
 |\tilde{x}_{i,j}\rangle &= \frac{1}{(1-p)^{1/(K_2-K_1-1)}} \frac{Ah}{j} |\tilde{x}_{i,j-1}\rangle, \quad 0 \leq i < m, K_1 + 1 \leq j \leq K_2 \\
 |\tilde{x}_{m,j}\rangle &= |\tilde{x}_{m,j_1}\rangle, \quad 1 \leq j \leq p
 \end{aligned} \tag{D10}$$

Therefore,

$$|x_{m,j}\rangle = \tilde{T}_{K_2}(Ah) |x_{m_1}, 0\rangle + \tilde{S}_{K_2}(Ah) h |b\rangle, \tag{D11}$$

where

$$\begin{aligned}
 \tilde{T}_{K_2} &= \sum_{k=0}^{K_1} \frac{z^k}{k!} + \frac{1}{1-p} \sum_{k=K_1+1}^{K_2} \frac{z^k}{k!} \\
 \tilde{S}_{K_2} &= \sum_{k=1}^{K_1} \frac{z^{k-1}}{k!} + \frac{1}{1-p} \sum_{k=K_1+1}^{K_2} \frac{z^{k-1}}{k!}
 \end{aligned} \tag{D12}$$

Our quantum circuit solves the linear system described by Eq. (D6). However, quantifying the operator norm between $C_{m,k,p}^{-1}$ and an errorless C_{∞}^{-1} , which is Taylor's series summed to infinity order, is meaningless because 1. $C_{m,k,p}^{-1}$ and C_{∞}^{-1} has different dimension. 2. The difference between them does not directly reflect the distance of the final state obtained by the algorithm. We therefore choose to follow the derivation in ref. [8] that evaluate the state distance between x^m and $x(mh)$. Equivalently, we are measuring the distance between the post-selected operator and an idea evolution on the target state. We will first prove the operator norm distance for T_k , followed by proving these distances can also upper bound the corresponding norm for S_k .

Let us first consider the truncation errors concerning T_k . We are going to derive $\alpha_1 = \|e^z - T_{K_1}\|$, $\alpha_2 = \|e^z - T'_{K_2}\|$, and $\beta = \|e^z - (pT_{K_1} + (1-p)T'_{K_2})\|$ for T_k , where

$$\begin{aligned}
 T_{K_1} &= \sum_{k=0}^{K_1} \frac{z^k}{k!} \\
 \tilde{T}_{K_2} &= \sum_{k=0}^{K_1} \frac{z^k}{k!} + \frac{1}{1-p} \sum_{k=K_1+1}^{K_2} \frac{z^k}{k!}
 \end{aligned} \tag{D13}$$

1. From the proof of Lemma 2, we can write $\alpha_1 \leq 2 \frac{(\ln 2)^{K_1+1}}{(K_1+1)!}$

2. Similarly, from Lemma 3, we can write $\alpha_2 \leq \left| -\frac{p}{1-p} \frac{(\ln 2)^{K_1+1}}{(K_1+1)!} + \frac{2}{1-p} \frac{(\ln 2)^{K_2+1}}{(K_2+1)!} \right| \approx \frac{p}{1-p} \frac{(\ln 2)^{K_1+1}}{(K_1+1)!}$

3. Observe that $pT_{K_1} + (1-p)T'_{K_2} = T_{K_2}$, $\beta \leq 2 \frac{(\ln 2)^{K_2+1}}{(K_2+1)!}$

As for S_k , we will prove three bounds on $\alpha'_1 = \|(e^z - 1)z^{-1} - S_{K_1}\|$, $\alpha'_2 = \|(e^z - 1)z^{-1} - S'_{K_2}\|$, and $\beta' = \|(e^z - 1)z^{-1} - (pS_{K_1} + (1-p)S'_{K_2})\|$, where

$$\begin{aligned} S_{K_1} &= \sum_{k=1}^{K_1} \frac{z^{k-1}}{k!} \\ \tilde{S}_{K_2} &= \sum_{k=1}^{K_1} \frac{z^{k-1}}{k!} + \frac{1}{1-p} \sum_{k=K_1+1}^{K_2} \frac{z^{k-1}}{k!} \end{aligned} \quad (\text{D14})$$

Consider

$$\begin{aligned} &e^z - T_k(z) \\ &= (e^z - 1) - (T_k(z) - 1) \\ &= (e^z - 1) - zS_k(z) \end{aligned} \quad (\text{D15})$$

Therefore, with $|z| \leq 1$, $\|e^z - T_{K_1}\| = \|(e^z - 1) - zS_{K_1}\| = \|z((e^z - 1)z^{-1} - S_{K_1})\| \geq \|(e^z - 1)z^{-1} - S_{K_1}\|$. S_k and T_k share the same bounds.

Theorem 7. Suppose V_1 and V_2 are quantum circuits solving the linear system in Eq. (D6) with $C_{m,K_1,p}(A)$ and $\tilde{C}_{m,K_1,K_2,p}(A)$ respectively. Solutions at time jh are denoted by x_1^j and x_2^j . We apply our framework $\mathcal{V}_{mix}(\rho) = pV_1\rho V_1^\dagger + (1-p)V_2\rho V_2^\dagger$ for a mixing probability $p \in [0, 1)$, and denote the obtained solution as $|x_{mix}^j\rangle$. We can upper bound the estimation error by

$$\| |x_{mix}^j\rangle - |x(jh)\rangle \| \leq \max \left\{ 8b, \frac{4}{1-p} a_1^2 \right\}, \quad (\text{D16})$$

where $a_1 \leq \frac{C_j}{(K_1+1)!}$, and $b \leq \frac{C_j}{(K_2+1)!}$. C_j is a problem specific constant.

Proof. Denote x_m^j as the state obtained by solving the linear system defined by $C_{m,K_2,p}(A)$. We have $a_1 = \| |x(jh)\rangle - x_1^j \|$, $a_2 = \| |x(jh)\rangle - x_2^j \|$ and $b = \| |x(jh)\rangle - x_m^j \|$.

By inserting bounds on α_1, α_2 and β into the proof of Theorem 6 in [8], we obtain that

$$a_1 \leq \frac{C_j}{(K_1+1)!} \quad a_2 \leq \frac{p}{1-p} \frac{C_j}{(K_1+1)!} \quad b \leq \frac{C_j}{(K_2+1)!}, \quad (\text{D17})$$

where $C_j = 2.8\kappa_V j (\| |x\rangle_{in} \| + mh \| |b\rangle \|)$, and κ_V is the condition number in the eigendecomposition of $C_{m,K,p} = VDV^{-1}$ for some diagonal matrix D . Further applying lemma 1, we can bound the state distance by

$$\| |x(jh)\rangle - |x_{mix}^j\rangle \| \leq \max \left\{ 8b, \frac{4}{1-p} a_1^2 \right\} \quad (\text{D18})$$

□

Appendix E: Simulation

We illustrate RTS by employing it in the Hamiltonian simulation with the BCCKS algorithm for the following Ising model with $n = 100$ and $t = 100$

$$H = \sum_{i=1}^n \sigma_i^x \sigma_{i+1}^x + \sum_{i=1}^n \sigma_i^z, \quad (\text{E1})$$

where σ_i are Pauli's operators acting on the i^{th} qubit and we choose to set all interaction and external field parameters to be 1 for simplicity. We can decompose Eq. (E1) into $L = 200$ Pauli operators, and the coefficient of each Pauli is

1. Thus, we must separate the simulation into $r = \sum_i \alpha_i t / \log(2) = 28854$ segments. We neglect that the evolution time for the last segment is less than t/r for simplicity.

For each segment, we need to perform 3(4) $\text{Select}(H)$ oracle and 6(9) Prepare oracle for each of $V_1(V_2)$ defined in Eq. (B8) and (B14). We also neglect any extra cost of implementing Hermitian Conjugate. Since the dominant gate cost is the $\text{Select}(H)$ we treat Prepare free. Each $\text{Select}(H)$ oracle can be implemented by $K(7.5 \times 2^w + 6w - 26)$ CNOT gates [33], where K is the truncation order and $w = \log_2(L)$. The CNOT gate cost for faithfully implementing the LCU algorithm at truncation K is thus well approximated by $G = 3rK(7.5 \times 2^w + 6w - 26)$. We define $\tilde{G} = G/(3r(7.5 \times 2^w + 6w - 26))$ as a cost indicator since it removes all constants. Note that implementing V_2 costs $4/3$ more than V_1 .

We traverse all combinations of $K_1 \in [1, 100]$, $K_2 \in [K_1 + 1, 100]$ and $p \in [0, 1]$ such that $pK_1 + (1-p)(4/3)K_2 = \tilde{G}$ and find the minimum ϵ using Eq. (B31) for each segment with a fixed cost budget \tilde{G} . We perform such calculation for $7 \leq \tilde{G} \leq 10$ and obtain the blue line in figure 1. The crosses with different colors indicate the achieved error and corresponding CNOT gate cost with discrete truncation, i.e. Eq. (B8) with \tilde{G} .

We denote V_{m,K_1,K_2} as the quantum circuit implementing RTS with K_1 and K_2 , and p will be a variable indicated in the axis. Similarly, V_{1,K_1} is the quantum circuit implementing the original LCU truncated at K_1 , and it is used to benchmark the performance of V_{m,K_1,K_2} . For figure 2, we calculate G for various truncations for V_{1,K_1} and V_{m,K_1,K_2} in different p . In the minor graph, we calculate the error for V_{m,K_1,K_2} and $V_{1,8}$ for $p \in [0.2, 0.999]$. By partitioning the calculation results, we can quantify the multiplicative impact of RTS on error reduction.